DIPLOMARBEIT

Titel der Diplomarbeit

„SCN9A and its natural antisense transcript"

Jennifer König

angestrebter akademischer Grad

Magistra der Naturwissenschaften (Mag.rer.nat.)

Wien, Oktober 2011

Studienkennzahl lt. Studienblatt:	A 490
Studienrichtung lt. Studienblatt:	Molekulare Biologie
Betreuerin / Betreuer:	Univ.Prof Dr.Juergen Sandkuehler

Table of Content

i. Abstract English

Pain is an essential part of our survival and keeps us in awareness of our physical limitations and protects us from harmful environmental stimuli. However pain and other somatosensory sub modalities like vision and smell are rather a perception, a product of our brain to handle and bring external sensory inputs to consciousness [10, 18]. Regardless of its essential role in one's survival, pain and in particular chronic pain which does not fulfil any physiological role, is a major clinical challenge to treat [15, 16]. Currently 10 % of the population are suffering from chronic pain due to irreversible nerve injury or inflammation. Up to now the two major classes of analgesics that are used to treat chronic pain (i.e. non-steroidal anti-inflammatories and the opioids) focus more on the symptoms of pain than its underlying causes. Recent scientific discoveries obtained from mice in knockout [31,32], knock down and overexpression studies as well as analyses of patients suffering from unusual pain states [20] show that voltage gated sodium channels are key players in several pain pathways.

In particular Nav1.7, a TTX sensitive voltage gated sodium channel that is mainly expressed in sensory DRG neurons and sympathetic ganglia neurons, is fundamental in initiation and propagation of action potentials [9- 21, 23] and plays an important role in pain sensation. Inherited or spontaneous mutations in SCN9A (Nav1.7) causing a gain of function result in hyperexcitability of DRG neurons and lead to Primary erythermalgia (PE) [12,14,21] and Paroxysmal extreme pain disorder (PEPD) while nonsense mutations causing loss of function of Nav1.7 cause Channelopathy-associated insensitivity to pain [20, 17].

Interestingly, SCN9A has a corresponding antisense transcript encoded on the opposite strand that tail to tail overlaps with the sense transcript and might play a role in regulation of SCN9A expression. Different studies have reported independently that natural antisense transcripts have an impact on the transcription level of its corresponding sense gene either through 1) interfering with its transcription 2) RNAi, RNA editing and RNA masking 3) or through epigenetic and chromatin remodelling [1].

By investigating the possible mechanism of SCN9A antisense transcripts on Nav1.7 expression, we aim to gain deeper insights into pain pathways and contribute to the development of a new specific class of analgesic drugs.

ii. Abstract German

Schmerz ist ein wesentlicher Bestandteil unseres Überlebens , er macht uns bewusst wo unsere körperlichen Limits liegen und schützt uns vor schädlichen Umwelteinflüssen . Schmerzen ,wie auch anderen somatosensorischen sub Modalitäten wie Sehen, Hoeren oder Geruch , eine Wahrnehmung, ein Produkt unseres Gehirns um externe Einfluesse zu verarbeiten und zu handhaben **(10) (18).** Abgesehen von seiner wesentlichen Rolle das eigene Überleben zu sichern , hat nicht jede Art von Schmerz und vor allem chronische Schmerzen eine funktionelle Rolle und stellt eine grosse Herausfroderung in der klinischen Behandlung da **(15, 16)**. Derzeit leiden rund 10% der Bevölkerung unter chronischen Schmerzen aufgrund irreversibler Nervenverletzungen oder Entzündungen. Die beiden großen Klassen von Analgetika, die verwendet werden, um chronische Schmerzen (dh nicht-steroidalen Antiphlogistika und Opioide) zu behandeln haben sehr viele Nebenwirkungen und ziele nur auf die Bekaempfung der Symptome ab, anstatt die zugrunde liegenden Ursachen zu behandeln. Neue wissenschaftliche Erkenntnisse durch Knockout **(31,32)** , knock down und Überexpression Studien sowie Analysen von Patienten mit ungewöhnlichen Schmerzzustaenden **(20)** haben zeigt, dass Natriumkanäle Hauptakteure der Schmerzweiterleitung und Prozessierung darstellen.

Insbesondere Nav1.7, ein TTX-empfindliche spannungsabheangiger Natrium Kanal, der hauptsächlich in sensorischen DRG-Neuronen und sympathischen Ganglien Neuronen exprimiert wird , ist von grundlegender Bedeutung in Initiation und Ausbreitung von Aktionspotentialen **(9 - 21, 23)** und spielt daher eine wesentliche Rolle im Schmerzen empfinden . Vererbte oder spontane Mutationen in SCN9A (Nav1.7), die zu gain of function Mutationen in Nav1.7 fuehren und in Hypersentitivteat von DRG-Neuronen resultierien, fuehren zu Krankheitsbildern wie Primary erythermalgia (PE) **(14,12,21)** und paroxysmale extreme Schmerzstörung (PEPD). Nonsense-Mutationen führen zum Verlust der Funktion von Nav1.7 und resultieren in Ionenkanal-assoziierten Unempfindlichkeit gegen Schmerzen **(20,17).**

Interessanterweise hat SCN9A ein correspondierendes Antisense-Transkript auf dem gegenüberliegenden Strang, das tail to tail angeordent ist und moeglicherweise eine Rolle in der Regulation der Expression SCN9A spielt. Verschiedene Studien haben unabhängig

voneinander gezeigt, dass Antisense-Transkripte Auswirkungen auf die Expression des sense Transkription des entsprechenden Gens haben, entweder durch 1) störung seine Transkription 2) RNAi, RNA-Editing-und RNA-Maskierung 3) oder durch Epigenetics und Chromatin-Remodeling . **(1)**

Durch die Erforschung des Mechnisms durch welchen SCN9A antisense transcript sein korrespondierendes sense Gene reguliert , erhoffen wir uns einen tieferen Einblick in die molekuaren Zusammenheange die unsere Schmerempfindung beeinflussen und steuern.Desweitern erhoffen wir uns dadurch wesentlich an der Entwicklung einer neuen Klasse von Schmerzmitteln beizutragen.

1. Introduction

1.1 Pain perception – Nociception

Pain is like other sensory sub –modalities a perception but in comparison to colour perception, pain does not only have a perceptual component but also highly psychological and cognitive components **(10)**. In other words, our internal pain scale or how we rate pain can change due to severe injury and might influence how we experience pain in the future. **(60)**. By contrast, pain research in the last couple of years suggests that our internal pain scale is based on our genetic background. In particular, research in the field of nociception and voltage gated sodium channels has brought evidence that even single nucleotide polymorphisms (SNP) or spontaneous point mutations in these channels can have a significant influence on pain thresholds and our internal pain scale **(20).**

A more generalized definition of what pain is comes from the International Association for the Study of Pain (IASP) defining pain as "an unpleasant sensory and emotional experience associated with actual or potential tissue damage, or described in terms of such damage" (http://www.iasp-pain.org).

What is undisputable is that pain is a crucial, non-redundant part of our survival, showing us our limits and protecting us from greater harm. This becomes even clearer in patients affected by congenital inability to experience pain **(20)**, not feeling any pain at all leads to severe injuries and consequently can reduce one's life expectancy dramatically. Although pain is fundamental, chronic inflammatory pain instead does not fulfil any protective purpose and strongly decreases a patient's quality of life. **(15)**

1.2 DRG neurons: primary afferents and transduction

Nociceptor. Pain sensation is mediated by a special subset of sensory neurons, called nociceptors that innervate the tissue with its bare nerve endings. Nociceptors are activated through environmental stimuli such as heat, cold, and chemicals. Activation leads to structural changes with corresponding opening and closing of ion channels and subsequent alteration of physiological and electrical properties of these channels. The main classes of

nociceptors can be distinguished by their afferent fibres, activating stimuli and distribution in skin and deep tissue **(18).** The two main classes of afferent fibres are slowly conducting unmyelinated C fibres and fast conducting thinly myelinated Aδ fibres **(10).** Conduction velocity differs between these two fibre types and they are also associated with different types of pain sensation.

First and second pain. In comparison to other somatosensory receptors like mechanoreceptors that terminate in specialized structures, nociceptors that mediate pain sensation end in bare nerve endings **(10).** Fast conduction Aδ fibres have a conduction velocity of 5- 30 m/s and are involved in first pain sensation, a rapidly perceived pain that carries information about what and where an incident happened. By contrast 2nd pain is much less informative and discriminative than 1st pain. It is mediated by slowly conducting unmylinated C fibres with a conduction velocity of 1m/s **(18).**

DRG neurons, most of which are nociceptors are pseudo unipolar neurons with their axons dividing into classic T junctions with peripheral and central branches. The peripheral branch consists of free nerve endings, mainly unmyelinated C fibres that innervate the tissue while the central branch projects its axon to 2nd order neurons in the spinal cord **(10).** Cell bodies of nociceptors are found in the dorsal root ganglia and vary in size, sets of channels expressed and gene expression. Among a variety of other channels, ion channels like the TRP (transient receptor potential) family are found on the axon tip of afferent fibres and respond to noxious stimuli such as acid, heat, cold and eicosanoids **(15).**

In the presence of a noxious stimulus these ion channels open and create a receptor potential that leads to a depolarization of the membrane. Additionally voltage gated sodium channels like Nav1.7, Nav1.1, Nav1.6 and Nav1.8 are also found near the peripheral terminals of nociceptors and activate when a certain threshold is reached. Mainly the activation of Nav1.7 voltage gated sodium channels contributes to initiation and propagation of action potentials **(28).**

2.   Transmission

2. 1   Voltage gated sodium channels – Introduction

Sodium channels are integral membrane proteins containing 4 homologous domains each of which consists of 6 transmembrane segments (S1 to S6) (20, 11) that form voltage sensitive and ion selective pores (21). These alpha subunits are connected to each other via intracellular and extracellular loops (11, 28). The sodium channel's voltage sensor is found in the S4 alpha helix in each of the four alpha subunit domains (I-IV) (11, 20). Voltage sensor residues in S4 are either lysine or arginine that are arranged in an interval of every 3rd amino acid, allow only positively charged Na+ ions and only at an appropriate membrane potential to enter through the pore by opening or otherwise closing the channel pore (21).

The molecular weight of the alpha subunits is around 220- 260 kDa and each voltage gated sodium channel is associated with auxiliary beta subunits. Four different beta subunits (β1, β2, β3, β4) have been identified (19, 21, 25). Beta subunits are single transmembrane proteins with an intracellular and extracellular binding domain. Interestingly the extracellular domain of β- subunits is homologous to a V-set (Ig-related domains of non-Ig molecules are described as being V -like when they are have a pattern of β-strands: V and V-related domains have about 65-75 amino acid residues between the conserved disulphide bond, and there are four β-strands in each β-sheet plus a short β-strand segment across the top of the domain, (22)) of Ig superfamily like adhesion molecules. Still not completely understood is what function β subunits fulfil to modulate VGSCs. It is hypothesized that β subunits interact with the cytoskeletal and the extracellular matrix (21) via their V set Ig domain and thereby might play a role in stabilizing the Nav proteins in the membrane (19) or help to even guide Nav polypeptides to membrane sites (19,21,25). Moreover, studies using Xenopus laevis oocytes with human β subunits indicate that they even modulate the gating properties of the alpha subunit (13). Co-expression of certain α subunits with a specific auxiliary β- subunit has been shown to modulate sodium channel properties (13, 19) by changing activation / inactivation properties of VGSCs. For example, Nav1.2 co-expressed with β1A subunit leads to a 2.5 fold increase in sodium current density due to increased channel functionality (21, 25).

All nine pore-forming isoforms (Nav1.1 – Nav1.9) of the alpha subunits are encoded by different genes (9- 21, 13, 14) (see Table A). In particular Nav1.1, Nav1.2, Nav1.3 and Nav.1.7 are closely structurally and functionally related and are encoded by a set of four genes clustered in the chromosomal locus chr.2q24.3. Each of the nine sodium channel

isoforms has its own highly specific distribution pattern within the CNS and peripheral nervous system **(14)** *(Table A).* Nav1.7 is highly expressed in sensory DRG neurons and sympathetic ganglion neurons, Nav1.8 and Nav1.9 are primarily found in damage sensing DRG neurons and nerve fibres **(16, 25).**

In humans, voltage gated sodium channels are highly conserved and show 75 % primary sequence homology of the transmembrane and extracellular domains **(25).** Voltage gated sodium channels can be distinguished by their ability to respond to TTX, a tetrodotoxin from puffer fish which binds to the ion selective pore **(12).** Nav1.1 to 1.4 as well as 1.6 and Nav1.7 are TTX sensitive and respond to nanomolar concentrations of TTX while Nav1.5, Nav1.8 and Nav1.9 are even insensitive to micromolar concentrations of TTX **(21).**

Mechanism of Action

Voltage gated sodium channels mainly contribute to action potential generation and propagation. Through their voltage sensor and ion-selective pores they allow the rapid influx of Na+ ions during the upstroke of an action potential **(9, 13, 14, 15, 16).** Structural conformation of voltage gated sodium channels changes with changing membrane potential and can either be (a) open (active state), induced via membrane depolarization; (b) fast inactivated, which occurs when the cytoplasmic loop binds to the pore of the VGSC to terminate the sodium flow and leads to (c) closed state: repriming (recovery from inactivation), which occurs while the membrane potential is repolarizing to get back to the resting membrane potential at -80mV **(13).** This simplistic view of Nav1 open and closed states has been proven to not hold entirely true for all voltage gated sodium channels. In particular VGSC found in DRG neurons, where a heterologous set of different sodium channels is present, show a more complex pattern of expressing currents. Patch clamp experiments with VGSCs identified sodium channels to be either sensitive or resistant to TTX. TTX sensitive VGSCs are rapidly inactivating while TTX resistant sodium channels slowly inactivate and might serve to prolong the action potential duration due to the longer open state of the channels leading to increased neurotransmitter release at the nerve terminals **(13, 14).**

2.2 Nav1.7 a hot spot for human pain disorders

SCN9A encodes for the alpha subunit of the TTX sensitive voltage gated sodium channel Nav1.7 **(9, 16, 20)** which is mainly found in slowly conducting **(13)** small diameter DRG neurons and sympathetic ganglion neurons. Nav1.7 is also very weakly expressed in the CNS **(31).** Immunohistochemistry with a specific antibody against Nav1.7 located the sodium channel at distal ends of neuritis. Human Nav1.7, (gene symbol SCN9A) is encoded on chromosome 2q24.3 and is a 113 kb gene that is comprised of 26 exons which are translated into a 1977 amino acid long polypeptide. Nav1.7 is crucial in initiation and propagation of action potentials **(9-21, 23).** Interestingly Nav1.7 is also found in olfactory sensory neurons and seems to connect the two sensory modalities, smell and pain. Patients suffering from Channelopathy-associated insensitivity to pain and anosmia have loss of function mutations in Nav1.7, causing the compromised function of nociceptors and olfactory neurons. **(27)**

2.2.1 SCN9A protein structure - See Fig2. and supplemental data 1

- SCN9A primary amino acid sequence is 1977 amino acids long.
- Ion selective pore: a re- entrant loop between helices S5 and S6 is embedded into the transmembrane region of the channel to form a narrow, ion selective filter at the extracellular end of the pore **(35).**

  In ion Trans I: AS 356 - 365

  In ion Trans II: AS 911 - 920

  In ion Trans III: AS 1390 - 1399

  In ion Trans IV: AS 1682 - 1691
- Transmembrane regions
- Coiled coil region AS 402 - 449
- Sodium Ion transport associated domain   AS 969 – 1191
- IQ AS 1877 – 1899
- Exon 5 has an alternative splicing variant **(57)**

  YLTEFVNLGNVSALRTFRVLRALKTISVIP

  YVTEFVDLGNVSALRTFRVLRALKTISVIP

- IFM Motif AS 1461 – 1463 , IFM motif and the charged residues in the domain III-IV linker identified to be critical for the fast inactivation kinetics of the rat brain II channel **(36)**
- Tetrodotoxin sensitivity defining amino acid AS Y362 **,** if this AS is mutated into a Serine it turns the channel into a TTX resistant one **(37)**

2.2.2 Nav1.7 electrophysiological properties

The Nav1.7 voltage gated sodium channel is highly sensitive to TTX and is predominantly found in C fibre axons of slowly conducting nociceptive DRG neurons and sympathetic ganglion neurons. Nav1.7 rapidly activates and inactivates from the open state within less than a millisecond **(28)** but, unlike other TTX sensitive VGSCs **(12)** it slowly recovers from fast inactivation (closed state inactivation) **(12, 13).** By slowly transiting to the closed inactivated state, Nav1.7 remains available for activation even with small or through slowly depolarizing potentials and serves as a threshold channel for Nav1.8 activation by amplifying incoming smaller current. In contrast Nav.1.8 voltage gated sodium channels only open at depolarization thresholds higher than Nav1.7 and is responsible for most of the inward current in the upstroke of action potentials **(14).**

2.2.3 Nav1.7 and inflammation

Nav1.7 is associated with inflammatory pain that occurs in response to prior tissue damage. Inflammation of the injured tissue leads to hypersensitivity in and around the affected area. Inflammatory mediators such as 5HT, prostaglandin and adenosine are released during acute tissue damage, **(10)** enhancing the magnitude of the voltage dependent Nav1.7 sodium current and shifting the Nav1.7 activating threshold to more hyperpolarized potentials. This increases the rates of activation and inactivation dramatically and in a second instance leads to increased sensitization of the nociceptors and the inflamed tissue **(14).** Hypersensitivity by increased excitability of a specific set of nociceptive neurons promotes healing and repair **(12).** Furthermore, CFA induced inflammation in mice leads to an up-regulation of Nav1.7 expression and increased amount of SCN9A transcripts **(30).**

Nociceptor-specific Nav1.7 k.o **(31)** and double k.o of Nav1.7 and Nav1.8 **(32)** confirmed Nav1.7's important role in the development of inflammatory pain. Interestingly, both the Nav1.7 k.o. and the double k.o. are still able to develop neuropathic pain. However, global k.o of Nav1.7 in mice is lethal which is likely to be related to the importance of Nav1.7 to the sense of smell **(29).**

2.2.4   Nav1.7 mutations and inherited human pain syndromes

Nociceptive pain primarily functions in detection and protection against potential or acute noxious stimuli such as heat, chemical injury, nerve damage and myocardial ischemia that causes severe damage, and induces a pain sensation that is highly unpleasant and not neglectable. Normally, nociceptive pain persists as long as the external or internal noxious stimulus is present. Nav1.7 is linked to three inherited monogenic pain disorders **(12).** Gain of function mutations can result in Primary erythermalgia or Paroxysmal extreme pain disorder which are characterised by intensely painful episodes **(13)** whereas homozygous loss of function mutations can result in a congenital inability to experience any pain at all **(20).**

2.2.4.1 Primary erythermalgia (PE)

Inherited autosomal dominant Primary erythermalgia is caused by missense gain of function mutations in SCN9A that lead to an increased activity of Nav1.7 due to altered electrophysiological properties. Mutations are found in the transmembrane domains and intracellular linker domains **(9)** some of which are in highly conserved parts of the channel (e.g. L858H) **(14)** *(Fig 1 overview, PE mutation).* All 14 reported PE mutations cause lowering of the channel's activation threshold. This leads to enhanced activity of Nav1.7 by shifting the voltage dependence of the channel to more hyperpolarized potentials. Moreover the majority of all reported PE mutations also affect the sodium channel's transition to an inactivated state (from open to inactivate). Normally Nav1.7 is a fast activating and inactivating channel but certain mutations result it in staying open for longer, leading to a larger inward current. Other mutations like I136V, L858F, A863P and F1449V, additionally speed up the voltage gated channel's repriming (recovery from inactivation).

Also a correlation between certain mutations and age of PE onset has been determined. Mutations such as I848T are linked to early onset of PE while others like Q10R are linked to late onset which only leads to a small shift in activation threshold toward more hyperpolarized membrane potentials.

Clinical symptoms characteristic for PE: First clinical symptoms in patients suffering from PE appear in the first decade of their life with reddened feet and hands due to moderate physical exercising, exposure to warmth and/or after long periods of standing **(14).** In the later course of PE, there are episodes of persistent burning pain and redness of lower extremities which can extend to the upper legs, feet, and often hands which is accompanied by elevated temperature of the affected areas **(9, 14).**

2.2.4.2 Paroxysmal extreme pain disorder (PEPD)

PEPD is an inherited autosomal dominant disease characterized by sudden onset and reoccurring episodes of burning pain in different body parts. PEPD is caused, similar to PE, by mutations in SCN9A that lead to a gain of function in Nav1.7 *(see fig1 overview PEPD mutations).* In comparison to PE, all mutations that are found in Nav1.7 evoking PEPD **(14, 28)**, do not enhance the voltage gated sodium channels activation but instead they impair its voltage dependent steady state inactivation. Most, but not all of the reported mutations that cause paroxysmal extreme pain disorder, shift the steady state inactivation to a more depolarized potential. This leads to incomplete inactivation of Nav1.7 **(15)**, and decreases the actual threshold for initiation of the action potential and increases the number and duration of evoked AP in DRG neurons leading to hyperexcitability of these neurons **(34).**

Clinical symptoms of PEPD: Patients with PEPD suffer from excruciating painful episodes that primarily affect the rectal, submandibular and ocular regions. **(14).** Patients with PEPD are strongly affected during their childhood with reoccurring and stronger painful episodes, **(34)** often accompanied with non-epileptic seizures and cardiac symptoms **(14, 29, 34).** Interestingly in most individuals, PEPD symptoms diminish with age although there are a number of cases where PEPD was carried into their adulthood **(28).**

4 characteristic stages are defined in PEPD **(12, 14)**

1. Stage, directly after birth, new-born has red flushes all over the back, legs, and soles of the feet.
2. Stage, rectal pain, childhood: burning pain that suddenly appears and lasts for at least 1h. The burning pain slowly moves down to the lower extremities followed by red flushes on the soles of the feet, skin, scrotum, left and right foot and buttocks
3. Stage, Ocular pain pattern, childhood: sudden onset of acute burning pain that lasts for a couple of minutes, followed by sporadic redness of skin, in particular in the temporal region and eyelids.
4. Stage, paroxysmal pain

Painful episodes are induced by eating hot, cold or spicy food; and by sunlight and strong wind. It is remarkable that although Nav1.7 is widely expressed within the PNS, PE and PEPD both show a highly specific tissue distribution of symptoms **(14).** This strong variation among these two diseases gives rise to the idea that Nav1.7 is probably not the only, but definitely an important part in developing PE and PEPD.

2.2.4.3 Channelopathy-associated insensitivity to pain (CIP)

CIP is a very rare inherited autosomal recessive disorder caused by recessive loss of function mutations in SCN9A. First insights into this highly unusual pain state were obtained through analysis of three consanguineous families from Pakistan **(20).**
Due to the frameshift or the nonsense amino acid changes in either exon 10 (S459X), 13 (I767X) and exon 15(W897X) **(14),** SCN9A mRNA does not encode for a functional protein in these families. ***(For all reported mutation in SCN9A see Overview fig1 CIP).*** Most patients suffering from CIP are from consanguineous families and are homozygous for the same mutation in SCN9A **(9)** and are from birth insensitive to painful stimuli but still respond to light sensation of touch, warm, cold, proprioception and pressure **(20).** While nociception is completely lacking in these individuals, any other physical and mental deficiencies could not be found. Despite having quite severe injuries that mainly go unnoticed and suffering from anosmia **(27),** they have an otherwise normal development, intelligence and health **(20, 29).** What is still not completely understood is why global Nav1.7 k. o in mice is lethal but in humans loss of functions mutations causes channelopathy associated insensitivity to pain in

otherwise healthy individuals. One explanation is that new-born mice with loss of Nav1.7 function are not able to find their mother's mammary gland and die due to malnutrition. Interestingly mouse Nav1.7 shows a higher expression in the CNS compared to human Nav1.7, in particular in the brain nuclei such as the paraventricular hypothalamic nucleus and the supraoptic nucleus **(9).** Furthermore, variability in inter-human pain sensation can be caused by polymorphisms in SCN9A **(14).**

Fig1 Overview of all reported mutations in SCN9A causing PE (IEM), PEPD and CIP
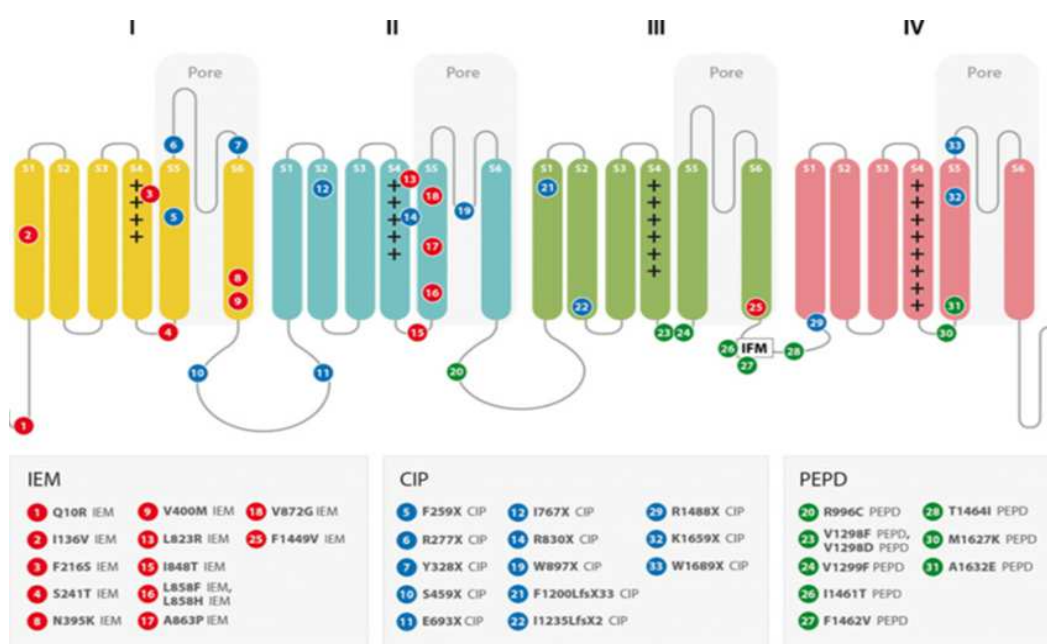
Fig1 Overview of reported mutations in SCN9A causing PE (IEM), PEPD and CIP (9)
Mutations reported in patients suffering from PE are found in the intracellular loops as well as in the conserved parts of the transmembrane domains of Nav1.7. PEPD mutations are mainly found in the intracellular linker regions. PE, PEPD are inherited autosomal dominant disorders whereas CIP is caused by inherited autosomal recessive mutations in SCN9A. PE enhances the channel activation, PEPD impairs Nav1.7 channel inactivation both leading to increased channel activity which is linked to hyperexcitability of DRG neurons.

2.2.5 Other voltage gated sodium channels and associated pain syndromes

2.2.5.1 Nav1.3 and neuropathic pain

Nav1.3 is a TTX sensitive voltage gated sodium channel mainly expressed in the adult central nervous system and during embryonic development. Its expression levels are normally very low in the PNS. Expression of Nav1.3 and β3 subunit in sensory but not primary motor neurons is only up-regulated due to nerve injury. Nerve injury also alters the level of neurotrophic factors like NGF and GDNF and reactivates the transcription of the normally transcriptionally silenced Nav1.3 VGSC **(30, 25).**

It was postulated that Nav1.3 up regulation might render DRG neurons hyperexcitable during nerve injury. This hypothesis was explained by Nav1.3 channel biophysical properties, fast inactivation after activation and fast repriming, while slowly inactivating from the closed state. The slow transition into a closed state, similar to Nav1.7, enables Nav1.3 to remain available for activation by small depolarizing potentials **(30, 25)**. However Nav1.3 global and DRG specific k.o. mice do not show any amelioration in pain behaviour after nerve injury and is therefore not responsible for the hyperexcitability of DRG neurons seen after nerve injury.

2.2.5.2 Nav1.8 inflammation and neuropathic pain

Nav1.8 is a TTX resistant voltage gated sodium channel which is mainly found in free nerve endings of DRG neurons and in trigeminal ganglia **(25).** Its location at free nerve endings enables Nav1.8 to strongly contribute to the level of neuronal excitability and modulate and influence pain signalling significantly **(21).**

Electrophysiological properties: Nav1.8 is a slowly inactivating (transition from open to closed state) and fast repriming TTXr channel thus activation and inactivation occurs at depolarized and voltage dependant potentials **(25).** Nav1.8 is the most significant VGSC in the depolarization phase of action potentials in DRG neurons.

Interestingly, inflammatory mediators like NGF influence the expression level of Nav1.8 and TTXR current levels while others like prostaglandin E2 and serotonin shift the channel activation to more negative potentials by phosphorylation of specific serine residues via intracellular 2nd messenger proteins PKA/C **(21, 25, 30).** This means that inflammation results in an increased activation and inactivation of the VGSC. Nav1.8 k.o mice confirmed

its contributory role in inflammatory pain and surprisingly also in cold evoked pain but no clear evidence for a role of Nav1.8 in neuropathic pain has been determined **(43).**

2.2.5.4   Nav1.9

Nav1.9 is similar to Nav1.8 as this channel is predominantly expressed in small diameter nociceptive DRG neurons **(25, 30).** In comparison to Nav1.8, Nav1.9 expresses a permanent TTX resistant current due to its activation and inactivation properties at hyperpolarized potentials, which are around the cell's resting membrane potential **(13).** The TTX resistant current expressed by Nav1.9 is mostly similar to the Nav1.5 cardiac current **(25).** Nav1.9 mainly contributes to the setting of DRG excitability by modulating the resting potential but due to its slow activating channel properties it does not engage in the depolarization phase of action potentials, like Nav1.8 does. Nav1.9 k.o and knock down mice treated with CFA expressed a reduced sensitivity to heat and mechanical pain suggesting a role for Nav1.9 in neuronal inflammatory pain, although there were no reported changes in Nav1.9 current properties **(54).** By contrast Nav1.9 k.o. does not influence acute pain and neuropathic pain thresholds.

2.3 Future prospective – a new desirable class of drugs

Currently two major classes of analgesics are used to treat chronic inflammatory pain: a) Non-steroidal anti-inflammatory drugs (taking hold through acting on arachidonic acid metabolism) and b) Opioids (acting on G proteins). However, these drugs can often be accompanied by severe side effects such as gastrointestinal bleeding (NSAIDs) and respiratory depression (opioids). Furthermore, the opioid class of drugs have issues associated with addiction and tolerance **(15)**. To understand how pain works and to design new classes of drug that specifically target the source of pain rather than just only treating its symptoms, it is crucial to understand how noxious stimuli are transduced, transmitted and processed within the PNS and CNS. Nav1.7 plays a key role in nociception and inherited pain disorders and mutations within this gene can have drastic impacts on pain sensation. Although Nav1.7 gain of function (PE and PEPD) and loss of function (CIP) mutations

cause a spectrum of human pain disorders and anosmia **(27)**, this voltage gated sodium channel does not seem to be involved in any other major pathway apart from pain and the sense of smell, which makes it an attractive target for a new class of analgesic drugs.

Table A: Overview voltage gated sodium channels (VGSC)

VGSC	Chrom.	Tissue	TTXs	Symptoms/Disease	Reference
Nav1.1	2q24.3	CNS/PNS	+	Epilepsy, Migraine	Dichgans et al 2005**(61)**
Nav1.2	2q24.3	CNS	+	Ko:Brainstem Apoptosis followed by severe Hypoxia,	Planell-Cases, 2000**(24)**
Nav1.3	2q24.3	Adult :CNS Low level in DRG Embryonic DRG	+	Up regulated in mice with normal acute and inflammatory pain	Nassar et al2006**(33)**
Nav1.4	17q23.3	Skeletal muscle	+	Hyperkalemic periodic paralysis	Lerhman-Horn et al., 2002**(26)**
Nav1.5	3p22.2	Heart/CNS	-	Visceral pain	Wilde et al 2011 **(65)**
Nav1.6	12q13.13	CNS	+	Impaired motor function	Levin et al2006 **(66)**
Nav1.7	2q24.3	DRG and sympathetic neurons	+	PEPD, PE , CIP ,chronic inflammatory pain Congenital pain disorder	Nassar et al 2004**(31)** ,Fertelman et al 2006 **(62)** Cox et al 2008**(20)**
Nav1.8	3p22.2	DRG	_	Cold pain , inflammation SNP in heart expressed Nav1.8 increases the risk of aterial fibrillation and heart attacks	Nassar et al 2005, Akopian et al **(64)**
Nav1.9	3p22.2	DRG	_	Inflammation	Priest et al 2005**(63)**

3. Natural antisense transcript (NAT)

The Human Genome Project offered a profound insight into how genomes are arranged and how little of its actual size consists of coding regions, suggesting that the complexity of life may not only lie within coding sequences. Technical improvements over the last decade led to the rather unexpected finding of extensive bidirectional transcription of eukaryotic genes. Some of these antisense transcripts result in pairs of sense and natural antisense transcripts that overlap and which maybe hybridise and even regulate each other's expression **(7).** Natural antisense transcripts or NATs are widely distributed throughout the human and mouse genome, but were first misinterpreted as transcriptional noise. The high number of NATs encoded in the genome suggests rather an evolutionary benefit from such a genomic arrangement. More evidence through high-throughput methods suggests a potential role of natural occurring antisense transcripts as transcriptional units like other regulatory RNAs **(2).**

3.1 Classification of NATs

Classification of NATs is related to their genomic location and their orientation to their corresponding sense transcript.

Classification according to their genomic location means that NATs are either in cis or trans. Cis-NATs are encoded on the same genetic loci and are perfectly complementary to the sense transcript. *Trans*-NATs are transcribed from different loci and are often shorter in size **(5)** and display an imprecise pairing with the sense transcript **(3).** A related class of transacting non coding RNAs are microRNAs and snoRNAs **(4).** Another approach to classify NATs applies to the orientation of the antisense transcript in comparison to the sense transcript. Possible genomic arrangements are (A) head-to-head 5'-5' or divergent NAT (B) tail-to-tail 3'-3'or convergent NAT (C) fully overlapping and (D) non overlapping NAT *(see Fig 3).* Regarding their encoded information, NATs can be protein coding containing an open reading frame or non–coding, with both variants having different regulatory potentials **(3).**

The length of natural antisense transcripts varies strongly between a 100 bp up to several thousand base pairs with a minimum sense overlap of 20 bp **(3, 7).** NATs are tissue and cell

specifically expressed but their expression level is often relatively low in comparison with their corresponding sense transcript which makes them quite difficult to detect and amplify **(5, 6).**

3.2 NAT detection strategies and pitfalls

Defining what is the sense and which one is the antisense gene occurs based on several key points that define the sense and antisense genes. A) if both transcripts are encoding a protein or if one is non-coding then the non-coding refers to the antisense gene B) expression pattern, the higher expressed gene is the sense copy C) mostly but not only the sense mRNA undergoes splicing and has longer intronic sequences.

Commonly used detection strategies to identify NATs are cDNA clones, EST libraries combined with exon – intron splicing sites and detection of poly a – tails. While the dominant fraction of NATs are nuclear restricted, non-coding and mostly not poly adenylated or spliced there are exceptions which are then excluded from detection methods using these criteria. Consequently the number of NATs is probably even higher than previously expected **(5).** Natural occurring antisense transcripts can also undergo splicing or arrive from intronless genes. Other pitfalls in detection of NATs and interpretation of high throughput screening and expression data arises also from varying NATs length for instance trans- NATs are commonly shorter **(5).** There is strong evidence that sense genes with an overlapping antisense transcript have a coordinated expression pattern which can be either positively or negatively regulated *Fig.2.* **(5, 6, 7)**

3.3 Antisense transcription

Approximately 15 to 20 % **(1, 2, 5, 6 7)** of all the coding mammalian genes and slightly less in plants **(7)** have an overlapping coding or non-coding natural antisense transcript **(5).** As NATs occur in such a high density throughout the genome then this implies an evolutionary benefit of such a genomic arrangement **(7)**. However, the evolutionary conservation of the NATs may not be primarily on the sequence level, as non-protein coding NATs genes have a quite a low conservation **(5)**. NATs are unequally distributed on the autosomes and X chromosomes, with underrepresentation of exonic overlapping NATs on the X chromosome which gives evidence to

evolutionary pressure on NATs. Regarding the common structural characteristics of NATs it points out that there is a conserved mechanism of regulation (6).

3.4 Functional and biological role of natural antisense transcripts

A clear advantage for RNA mediated transcriptional regulation is given by its quick production and degradation, its local storage, conformational flexibility, distribution, and its ability to interact with both nucleic acid and protein (5). Furthermore by using RNA transcripts as intermediate transport and information forms, cells can precisely direct spatial and local expression of proteins. Natural occurring antisense transcripts provide a new level of RNA based transcriptional regulation that is distinct from the already known epigenetic mechanisms of regulating transcription such as DNA methylation and histone acetylation *(See Fig2).*

3.4.1 RNA–antisense RNA interaction: RNA editing, RNAi and RNA masking

3.4.1.1 RNA editing

After being transcribed from the DNA strand, pre mature RNA undergoes a variety of maturation steps, such as 5' capping, splicing and 3' processing and polyadenylation (40). Another post transcriptional mechanism is RNA editing. Several different types of RNA editing (39) are known which alter the target mRNA sequence by a) addition or deletion of nucleotides or b) changing one nucleotide to another (40). The most popular form of this post transcriptional site specific alteration is the conversion from A-> I (Adenosine to Inosine) in dsRNA through an enzyme called ADAR (adenosine deaminase acting on RNA). Inosine base-pairs with cytosine and is functionally equivalent to guanidine (38).
Adenosine deaminase acting on RNA (ADAR). RNA editing occurs only in dsRNA although the length of the ds region that is targeted by editing can vary. Three different ADAR enzymes (ADAR1, ADAR 2 and ADAR3) are found in humans and are widely present throughout different tissues, except for ADAR3 which is only found in the CNS. Within a cell ADAR1 and ADAR2 have a specific subcellular distribution, ADAR1 and its 2 isoforms ADAR1L (long splicing transcript) found in the cytoplasm and ADARS (short splicing transcript)

present in nucleolus and nucleoplasm whereas ADAR2 is found only in the nucleolus. This distinct cellular distribution gives an idea of where the substrates they recognize are located **(40).** ADAR mutation or alterations in the RNA editing machinery are also linked to a various human diseases, such as depression, ALS, neuronal apoptosis and Dyschromotosis symmetrica hereditaria **(38, 42).**

RNA editing and natural antisense transcripts. The biological role of RNA editing lies in fine tuning protein function, RNAi , modulating neuronal signals and control of microRNA function **(38,40)**. Through RNA editing genetic diversity is created, one gene can give rise to a set of slightly different proteins while not abandoning the original one. But for one gene or mRNA to be edited by ADAR it must be present in a double stranded structure, either through forming a loop within its own structure or by nuclear duplex formation with its corresponding antisense transcript **(44)**. Most of the reported A-to I editing sites are found in Alu repeats and long interspersed elements (LINES), which are mainly located in untranslated UTR regions of the mRNA **(40).** It was hypothesized that sense and antisense transcripts may form a nuclear RNA duplex that can serve as substrate for the RNA editing machinery, leading to the degradation, nuclear retardation or creation /destruction of splicing sites within the sense transcript **(1).** *Rnp4f* gene and its correspondent NAT *Sas10,* is a prominent RNA editing case reported from Drosophila melanogaster where a sense antisense pair undergoes RNA editing **(44).** However there is no evidence yet supporting a role of RNA editing in human and mouse sense-antisense pairs **(1).**

3.4.1.2   RNAi

RNAi is a highly conserved response and defence mechanism against dsRNA that triggers sequence specific post transcriptional silencing. RNAi therefore acts as an antiviral defence, influences gene regulation and genomic stability, protects against transposons and inhibits genomic rearrangements during differentiation.

SiRNA and miRNA. Although they share one common feature i.e. their length (~20 -24nt), siRNA and miRNA differ strongly in their origin and regulatory function**.** SiRNA derives from viral DNA and transposons and are transcribed by RNA polymerase II, and exported into the

cytoplasm. MiRNA derives from genomic sequences and are transcribed by RNA polymerase III. Pri-miRNA is processed by Drosha and also exported into the cytoplasm.

In the cytoplasm an RNA III nuclease, DICER, binds to the dsRNA molecules, unwinds and cleaves them into small RNAs. The passenger strand is degraded, while the small RNA accumulates and is recruited by RNA induced silencing complex, RISC (53). RISC incorporates the ssRNA molecule and induces siRNA gene specific silencing. MiRNA can also induce gene specific silencing, while also target other genes at the same time, or regulate gene expression. SiRNA are homologous to their target RNA while for miRNA the degree of target complementarity determines its function, either as a silencer or a transcriptional regulator (40).

RNAi and NATs. It has been suggested that sense and antisense RNA duplexes may be processed by Dicer and mediate RNA induced silencing. Evidence for this RNAi mediated NAT mechanism is by now only proven to occur in *Arabidopsis* where salt tolerance is regulated by siRNA formation which is encoded by a pair of tail to tail overlapping sense and antisense pairs. But here both sense and antisense transcripts are coding for two stress related genes P5CDH (sense) and SRO5 (antisense). P5CDH is expressed under normal physiological conditions. Due to altered salt concentration the transcription of SRO is induced leading to duplex formation of sense and antisense transcripts and down regulation of P5CDH through cleavage of its mRNA. There have not yet been any reported cases of RNAi- NAT mediated regulatory mechanisms in mammals. (1).

3.4.1.3 RNA masking

Unlike RNA editing that occurs in the nucleus, RNA masking takes place in the cytoplasm (44). Sense and antisense RNA or more general ssRNA folds up into hairpin structures and masks binding sites for transcription factors or miRNA, splicing sites or influences the stability and translation of the sense mRNA (1).

Prominent examples for RNA masking. BACE1 (β site - amyloid precursor protein cleaving enzyme) which is involved in Alzheimer's disease, shows an increased stability when its corresponding antisense transcript is present (8). Through duplex formation with BACE1 antisense transcript, a miRNA binding site is masked (45). Another well studied example of

RNA masking is the HIF (hypoxia inducible factor) that is activated due to low oxygen conditions. Two main splice variants of HIF-1α and HIF-2α are known, they show distinct functionality during embryogenesis **(46)**. The expression of HIF1-α antisense transcript alters the mRNA stability of one splicing variant dramatically by altering its 2nd structure and exposing an Alu rich element and leading to its decay **(44, 45).** Recent findings discovered that p53, the main tumour suppressor and guardian of the genome whose loss of function is a major cause of cancer, has a corresponding antisense Wrap53. Wrap53 stabilizes p53 mRNA leading to an increase in both mRNA and protein levels of endogenous p53. Protein levels are enhanced by Wrap53 targeting the 5' untranslated region and marking it for siRNA **(45,48)** RNA masking which results in correlated expression levels of sense and antisense transcript **(1)** *See figure 2 (B).*

3.4.2 DNA–RNA interactions: transcriptional interference, epigenetics

3.4.2.1 Transcriptional interference

Transcriptional interference is based on the assumption that transcription occurs only in one direction at a given time **(44).** As sense and antisense transcripts are encoded on opposite strands, RNA Polymerase II simultaneously transcribes from each strand but the transcriptional apparatus might collide in the overlapping regions **(1).** Transcriptional interference leads to either a non-correlated, inverse expression pattern or a complete stop of transcription on both strands. A study on the effect of length and type of the overlap of sense-antisense genes on their expression level found a correlation. The length of the overlapping regions that were up to 200bp showed the highest sense and antisense co-expression whereas co-expression decreased to zero at overlapping lengths >2000bp. This proves the longer the overlap the more likely is transcriptional collision. Head to head, tail to tail and fully overlapping are the three types of orientation of sense and cis NATs. The way they are oriented to each other has also an impact on their expression level like length does. Head to head orientation and fully overlapping NATs show a decreased co-expression pattern than tail to tail sense–antisense orientated NATs **(47).**

Prominent examples of transcriptional interference: Gal7 and Gal10.

Due to transcriptional collision of RNA Polymerases II in the overlapping area, sense and antisense transcripts exhibit an inverse expression pattern *see fig2 (A)* **(1).** What is still controversial is the role of transcriptional interference as the main regulatory mechanism for NATs. First this approach requires that sense and antisense RNA are transcribed simultaneously from only one allele. This is often not the case either and the time point of transcription can vary between sense and antisense transcripts or the transcript from different alleles, maternal or paternal. This might explain why the X chromosome shows relatively low levels of antisense transcription (i.e. gene dosage, one X chromosome is inactivated) **(44).**

3.4.2.2 Chromatin remodelling and epigenetics

Chromatin remodelling is induced by altered methylation, acetylation or phosphorylation states leading to chromatin decondensation or condensation, which makes certain genes accessible or inaccessible for transcription. It has been suggested that NATs play a role in DNA methylation by directly interacting with methylases or influencing chromatin modifications of non-imprinted autosomal genes by recruiting histone modifying enzymes **(44).** The proposed mechanisms by which NATs alter expression and influence chromatin condensation, is through suppressing transcription of the sense gene by binding to its promoter region and in a 2nd instance recruiting histone remodelling enzymes, like deacetylases and methylases **(1, 44).** Several well characterized cases of NAT mediated transcriptional silencing are reported, where binding of antisense to regulatory DNA sequences induces trimethylation and heterochromatin formation **see fig 2 (D).**

For example, CDKN1A (p21) encodes for a cyclin dependant kinase inhibitor which is a well-known tumour suppressor gene that is regulated by its corresponding antisense transcript. CDKN1A antisense expression recruits and mediates trimethylation at the sense promoter region. Highly interesting in this case, is that a synthetic 21bp long dsRNA targeting the p21 promoter region causes a phenomenon described as RNAa (RNA activation) leading to p21 expression **(52).**

Through Dicer k. o. studies, where heterochromatin formation was drastically impaired, it was proposed that RNAi and chromatin remodelling might work in concert **(51).** More

evidence supporting a role for NATs in epigenetics is based on the finding that chromatin binding enzymes have conserved RNA binding motifs, giving rise to the idea that NATs are local modulators of chromatin remodelling enzymes. Another very interesting aspect is that NATs have a relatively low expression level but their impact on sense expression can be dramatic, suggesting epigenetics as a central mechanism of NAT mediated transcriptional regulation due to its low copy number requirements. There are only two alleles of each gene in a given healthy cell, if NATs directly interact with DNA, then theoretically only 2 NAT copies per cell would be required to suppress or modulate gene expression **(44)**. Moreover, antisense expression reaches its peak before and during recombination and is believed to induce opening up of chromatin structures during recombination **(1).**

Genomic imprinting describes the phenomenon of an inherited monoallelic expression, where either the maternal or paternal allele of a gene is expressed. Around one hundred and sixty imprinted genes are reported most of which are found in small clusters **(53).** For several cases of genomic imprinted genes, chromatin remodelling and DNA modifications are induced by natural antisense transcripts **(6, 7, 8, 44).**

Prominent example: X chromosome inactivation. X chromosome inactivation is required to regulate gene dosage in female mammals. First during an early stage of embryonic development, only the paternal X chromosomes are inactivated which is reversed in the early blastocyst. One of the two inherited paternal or maternal X chromosomes will be randomly inactivated during embryogenesis. X inactivation, the transition from eu- to heterochromatin that is firmly packed, is controlled by the *Xic* (X inactivation centre) where four non protein coding genes are found. The *Xic* is crucial for X inactivation and encodes *Xist, Tsix, Jpx* and *Ftx.* Xist, a long non coding RNA is weakly expressed from both X chromosomes but is relatively unstable **(50, 44)**. Due to changes of either stability or to sex specific induction of transcription the expression level of *Xist* increases from the prospective inactive chromosome, *Xist* spreads, binds and coats the future inactive chromosome **(55).** Further *Xist* coating recruits histone methylases and leads to chromatin condensation **(1).** On the same locus, on the opposite strand, downstream of Xist a natural antisense transcript *Tsix i*s encoded. *Tsix* is a non-coding 40 kbp long, nucleus restricted RNA that is also weakly expressed from both chromosomes before onset of X inactivation **(50).** While

the inactive X chromosome enhances *Xist* expression, the remaining active X chromosome increases the expression of its antisense gene *Tsix* **(1).**

Although it is still not fully understood through which exact mechanism natural antisense transcripts influence chromatin remodelling, in most cases the expression of a whole cluster of genes is altered. For chromatin remodelling, an inverse expression pattern between antisense transcript and all genes in the cluster is predicted **(1)** *see fig 2 (D)*
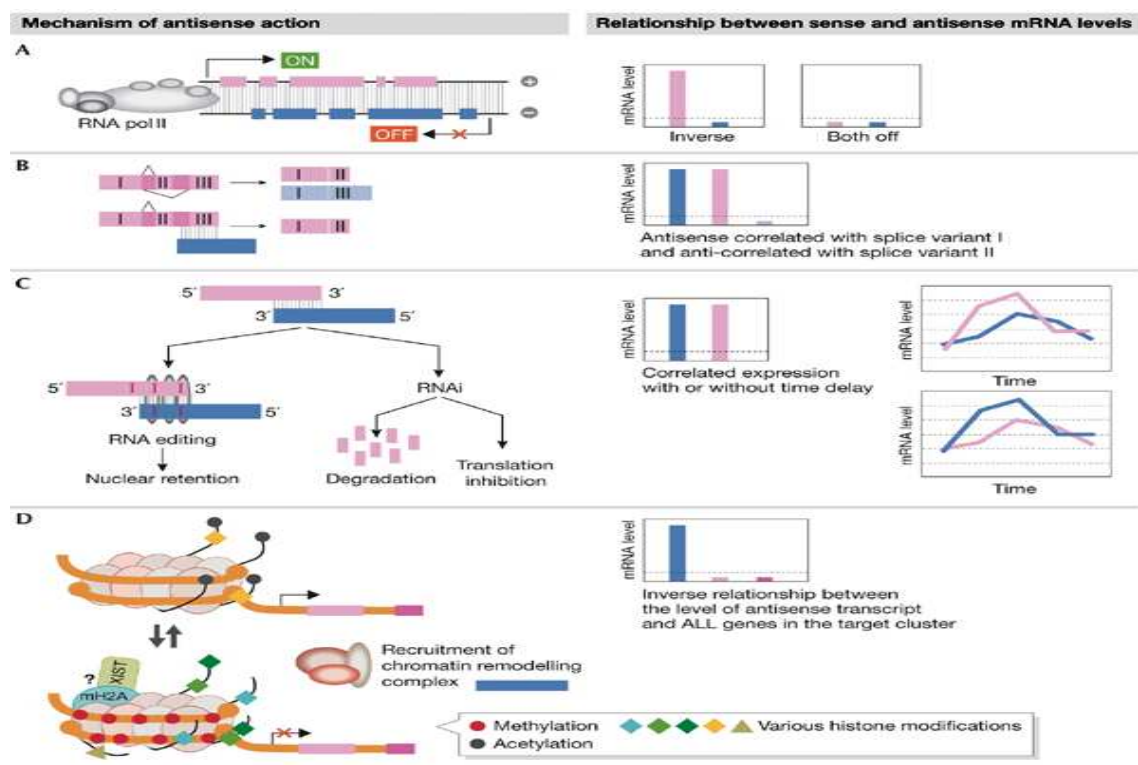
Fig.2 Left: OVERVIEW: Possible regulatory mechanisms by which NATs can influence expression levels of corresponding sense transcripts. Mechanism of antisense action (A) *Transcriptional interference* (B) *Alternative Splicing* (C) *RNA editing and RNAi* (D) *Chromatin remodelling* **Right: Relationship between sense and antisense mRNA levels** **(1)**

4. SCN9A and its corresponding antisense transcript

The human and mouse SCN9A/Scn9a sense genes both have a corresponding antisense transcript organised into a tail to tail arrangement (i.e. 3' ends overlapping). The sense-antisense overlapping region in human is approximately 500 bp while in mouse it is around

180bp. Both antisense transcripts in mouse and in human are non-protein-coding and have a total length of 2352bp and 1347bp respectively.
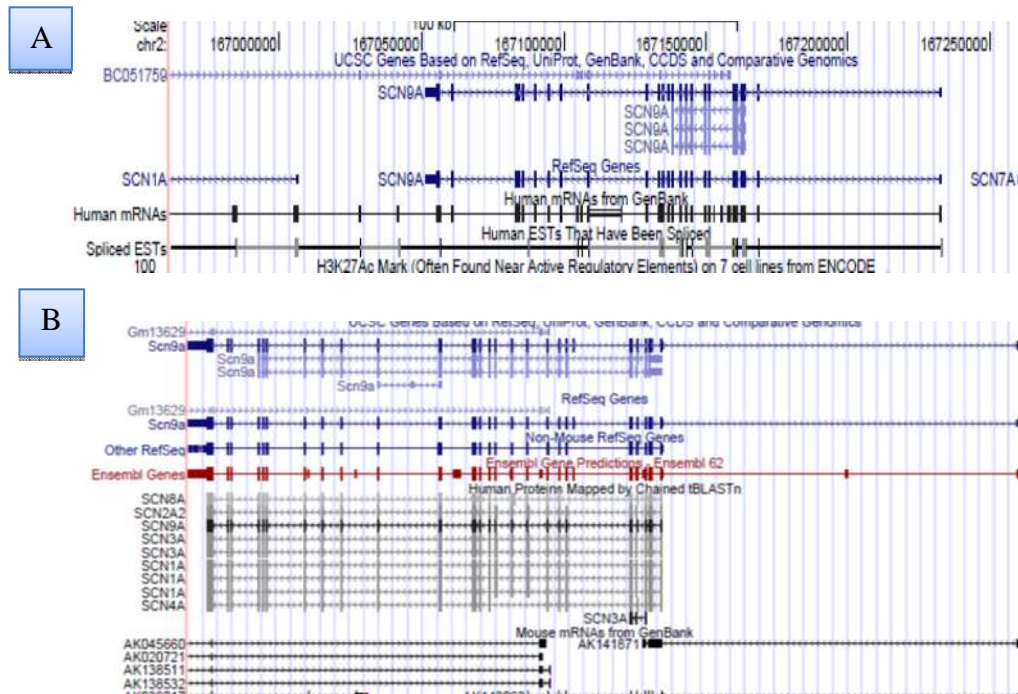
Fig.3 Natural *antisense transcripts and sense transcript can have four different genomic arrangements: head-to-head 5'-5', divergent NAT (B) tail-to-tail 3'-3', convergent NAT (C) fully overlapping (D) no- overlapping. A: Tail-to-tail arrangement of human Nav1.7 antisense gene (BC051759) and SCN9A on chromosome 2 (genome uscs) (B) tail to tail arrangement of the mouse SCN9a antisense gene on chr.2. Size of the sense-antisense overlapping region for mouse ~180bp while for human ~500bp.*

5.   Material and Methods

5.1   Gels, LB and Plates

5.1.1   Agarosis gel 0.9 %, 1.62 g agarosis in 180ml 1x TAE Buffer

5.1.2   1kb Ladder Invitrogen *see appendix AP 1.1*

5.1.3   100bp Ladder Invitrogen *see appendix AP 1.2*

5.1.4   LB 10 g LB broth in 500ml ddH20. Mixed by hand and autoclaved for 20 min at 121 degrees

5.1.5   LB Agar 10 g LB and 7.5 g Agar broth in 500 ml ddH20 autoclaved for 20 min at 121 degrees and cooled down to ~42 C

5.1.6   Antibiotics added to LB or LB+Agar Ampicillin (100ug/ml) or Kanamycin (25ug/ml)

5.2.   RNA isolation

Deeply anesthetize mice with CO_2 and terminate through neck breaking, dissect DRGs, and bring freshly dissected DRGs into RNA*later* (Qiagen 11560622) or dissection medium. Remove nerve strings and store for maximum one week in RNA*later* at 4C.

- Dissection medium: HBSS w/o Ca2+and Mg2+, HEPES (Gibco 15630-049) 5mM, Glucose 10mM (Sigma)

Clean glass homogenizer by washing with tap water and 1 time with RNaseZap (Ambion 9782) and three times with 1 ml of DEPC-treated water. Finally wash glass homogenizer with 0.5 ml of TRIzol. Add 0.6 ml TRIzol (Invitrogen 15596-026) into homogenizer and transfer dissected DRGs into the glass homogenizer. Mixture is left incubating 3-5 minutes at room temperature. DRGs and TRIzol are carefully homogenised by hand for at least 1-2 min but maximum 3 minutes. Sample volume of approximately 700ul is brought onto a QIAshredder mini column (Qiagen 79654). Spin full speed at 13k rpm for 2 min, column is removed and supernatant is centrifuged for another 3 minutes at full speed. Transfer supernatant into PLG tube (Phase-lock Gel, heavy (VWR 713-2536)). Spin at ~16,000xg for 20 seconds before use. Measure the volume of supernatant with a pipette. 2/10th of sample volume of chloroform is added to the sample (or chloroform isopropanol alcohol 24:1). Mixture is shaken vigorously by hand for 15 seconds and left to stand for 3 min. Spin (~16,000x*g*) for

15 min at 4ºC. Carefully remove the upper colourless aqueous layer using a p10 tip to recover the final drop, and place into a fresh 1.5ml tube. Measure the volume of this aqueous phase with a pipette. Slowly add an equal volume of 70% ethanol to the aqueous phase. Gently mix by pipette and transfer the sample to an RNeasy MinElute spin column (Qiagen 74204) place in a 2 ml collection tube. Close the lid and spin for 15 seconds at 16,000x*g.* Discard the flow-through. Place the RNeasy MinElute spin column in a new 2 ml collection tube. Add 500 µl Buffer RPE to the spin column. Close the lid and spin for 15 seconds at 16,000x*g.* Discard the flow-through. Pipette 80 µL of the DNase I/Buffer RDD mix onto the membrane, leave at RT for 15min. Close the lid and spin for 15 seconds at 16,000x*g.* Discard the flow-through. Add 500 µl Buffer RPE to the spin column again. Close the lid and spin for 15 seconds at 16,000x*g.* Discard the flow-through. Add 500 µl 80% ethanol to the spin column. Close the lid and spin for 15 seconds at 16,000x*g.* Discard the flow-through. Put the RNeasy MinElute spin column in a new 2 ml collection tube. Open the lid of the spin column, and spin at full speed for 5 min, put the RNeasy MinElute spin column (Qiagen 74204) in a new 1.5 ml collection tube. Add RNase-free water (Invitrogen) directly to the centre of the spin column membrane. Close the lid gently, and spin for 2 min at full speed to elute the RNA. Measure the RNA concentration with Nanodrop and store at –80 degrees.

5.3   Cloning, Kits and PCR

5.3.1   OneShot© Top10 chemically competent cells (Invitrogen C4040-10)
         For protocol *see Appendix AP1.3*

5.3.2   XL10-Gold ultracompetent Cells (Stratagene C- 200314).
         For protocol see Appendix AP1.4

5.3.3   Miniprep (**Qiagen Spin Miniprep kit). For protocol *see appendix AP1.5***

5.3.4   Maxiprep protocol *see appendix Qiagen High speed Maxiprep kit. For protocol see* Appendix AP1.6

5.3.5   Gel purification see appendix AP1.7 *Qiagen Gel purification kit*

5.3.6   PCR Purification *Qiagen see* Appendix AP1.8

5.3.7   DreamTaq Green DNA polymerase kit AP 1.16

5.4 Restriction digests

- **Single Digest**: 15 μL of H₂O, 2 μL of appropriate restriction enzyme buffer, 2 μL of DNA (200ng), 1 μL of restriction enzyme. Leave 3hours at 37°C or 65 °C
- **Double Digest**: for 2 restriction enzymes, use 1 μL of each enzyme with 2 μL of buffer, 2 μL of DNA (200 ng) and 14 μL of H₂O.

Enzymes used EcoRI, BamHIII, BstBI, BsaAI, KpnI, HindIII (New England Biolabs)

5.5 SuperScript RT (Invitrogen) see Appendix AP 1.9

5.6 Phusion high fidelity PCR kit, Finnzymes F-553S/L protocol see Appendix AP1 .10

5.7 Ear DNA Extraction for PCR – Isolation of Genomic DNA

Collect ear tissue in 0.5 ml tube using an ear puncher. If not extracting DNA immediately, store tissues in freezer. Prepare enough lysis mixture for all samples plus a bit extra (i.e. if you have 10 samples, make up enough for 11). The lysis mixture consists of PCR lysis buffer and Proteinase K 1/500 dilution. Add 30 μl of this lysis buffer mixture to each tube. Place tube in PCR machine and incubate at 55ºC for 1 h .Vortex halfway through the incubation to facilitate lysis. Incubate at 95ºC for 5 min to de-activate proteinase K. Add 30 μl of distilled water and vortex for 30 s. Spin at 12,000 rpm for 1 min. Use 1 μl of supernatant per PCR reaction. Store the DNA sample at -20ºC.

<u>PCR Lysis Buffer (stored at -20ºC)</u> 10X GB, 25% TritonX-100, beta-mercaptoethanol, H2O<u>10X GB (store at -20ºC)</u> 1.5M Tris pH8.8, 1.0M (NH4)2SO4, 1.0 M MgCl2, H2O

5.8 Mouse Total RNA Master Panel

Mouse total RNA master Panel (Clontech 636644 **see Appendix AP1.11**). Total RNA from BALB /c m/f mice isolated by a modified guanidinium thiocyanate method. Total RNA from 15 different samples of tissue and developmental stage specific RNA with a concentration of 1ug/ul. Total RNA is transcribed into cDNA with SuperScript *(see 5.5)* and cDNA is used as a template for PCR with proofreading DNA Polymerases Phusion *(see 5.3.7)*. Additionally one sample of black6 mice DRG cDNA (Black6 DRG) =110ng/ul is added to the mouse Total RNA master panel.

Primers for mouse tissue panel are chosen due to their efficiency in previous PCR reactions. Neat template is diluted ¼ in H20.

Nav1.7 sense primers M1.7 RXN 6 FWD 5'-GGCAAACTGACTACATGAGTTTTG-3', M1.7 RXN 6 REV5-'TGTAAACAGTGTATCAAAACCGAAGC-3'expected size 1375bp, which were also used during the RNA editing project. **Nav1.7 antisense primer**: M1.7 AS 1 FWD 5'-GAACCAGGTCTTGCTTTTCG, M1.7 AS 1 REV5'CCACGCTTTGTTCCTAGAGC-'3 expected size 625bp. **Housekeeping Gene HPRT1:** FWD 5'- GATGATGAACCAGGTTATGACC-3', REV 5 – TTTCCAGTTTCACTAATGACAC-3' expected size 605bp

PCR reactions were performed with proofreading DNA polymerases – i.e. Phusion *(see 5.3.7)*

ThermoCycling condition: Annealing temperature (Ta)

Ta (M1.7RXN 6) =63.3 C, 35 cycles; Ta (M1.7 AS 1) =63.5 C, 30 cycles; Ta (HPRT1) =55C 30 cycles; PCR with Phusion is performed at an annealing temperature +3C above the Tm of the primer used during PCR.

5.9 VECTORS

5.9.1A Cloning of human full length antisense transcript

Human, **BC051759,** cloning of the whole BC051759 sequence from a bought cDNA: IMAGE Human CDNA clone, BC051759 Clone ID 5582690. CDNA Image Human Clone arrived in a glycerol stock and was plated out onto LB Amp plates. Following incubation overnight, single colonies were inoculated into 5ml liquid LB + Ampicillin. DNA was then isolated using Miniprep protocol and used as template in PCR using Phusion. To obtain enough antisense transcript for cloning into pcDNA3 expression vector, at least 8 identical PCR reactions were started. Primer: Human AS HINDIII FWD 5'-CCCAAGCTTGTCTTAGTCCTCTGAATATTTT-3', Human AS KpnI REV5'-CGG GGTACC CCA ATTGATGGAGAATTTTAT-3' expected size of the PCR product 2302bp.

PCR reactions were loaded on a 0.9% agarosis gel and bands cut out under UV and pooled for gel purification. Human Nav1.7 full length antisense sample concentration measured via Nanodrop: c (H1.7AS): 98.4 ng /ul eluted in 40 ul Elution Buffer (Qiagen) (used as stock).

Fig 5.9a Human (A) *Amplification of full length antisense sequence from a cDNA clone using specific primers with integrated restriction sites* (B) *Double restriction digest with KpnI and HindIII*

5.9.1B Cloning of mouse full length antisense transcript

The mouse full length antisense transcript was cloned using a mouse cDNA clone as template (AK138532) (Fantom CDNA clone (http://www.dnaform.jp/products/fantom/pd^{A}f/FANTOM-PX-PY-PZ.pdf) **(see Appendix AP1.12)**. The cDNA clone stock (5 ng) was plated out onto LB+AMP plates and incubated o/n at 37 degrees. The following day, single colonies were inoculated into 5ml liquid LB + Ampicillin. DNA was then prepared using a Miniprep protocol and used as template in PCR using the Phusion proofreading DNA polymerase. To obtain enough antisense transcript for the following cloning step into pcDNA3, at least 8 identical PCR reactions were performed using the proofreading DNA Polymerase Phusion. Primer sequences: Mouse full- length antisense HindIII FWD 5'-CCCAAGCTT GAGCAAGAGT AAGAAGTA-3', Ms AS KpnI REV 5'- CGG GGTACC GCCATTATATTTCAT-3', expected size 1347bp **(full length antisense cDNA sequence see supplemental data 2).** PCR reactions were loaded onto a 0.9% agarosis gel and bands were cut out under UV and pooled for gel purification. Mouse Nav1.7 full length antisense sample concentration measured via Nanodrop: (Ms Nav1.7): 46.5 ng /ul eluted in 40 ul Elution Buffer (Qiagen)

For Both 5.9.1A and 5.9.1B

As the human and mouse full length antisense transcripts are non-coding and not translated into protein, precise cloning of the antisense transcript with as few as possible additional bases is required. Therefore human and Mouse full length antisense primers are designed to include specific restriction sites that map to the 5' end of the multiple cloning site to reduce the number of additional bases that could be transcribed from the pcDNA3 expression vector. Restrictions sites integrated into the primer sequence were chosen according to RestrictionMapper (http://www.restrictionmapper.org/). Browsing of both human and mouse SCN9A antisense transcript cDNA gave KpnI and HindIII as optimal cutters as they do not cut within the antisense transcripts but have cutting sites towards the 5' end of the multiple cloning site ofpcDNA3.
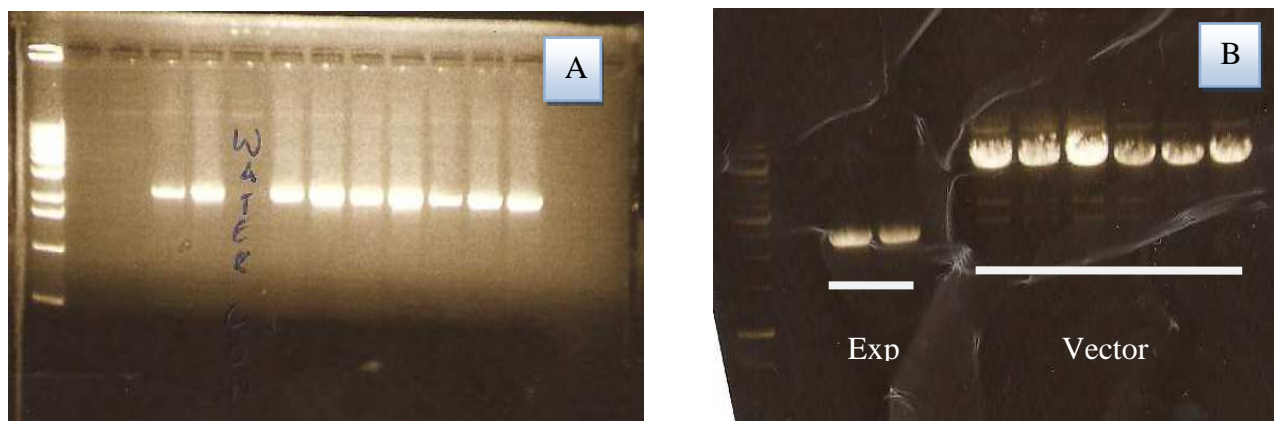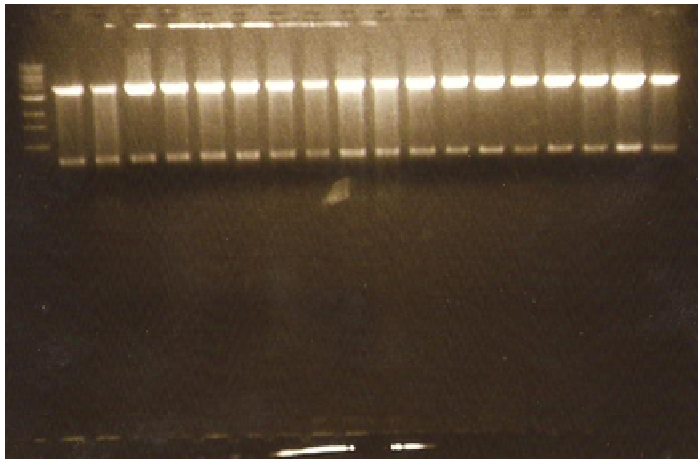

Fig5.9b Mouse (A) Amplification of full length antisense sequence from cDNA clone using specific primer with integrated restriction sites .Clear and strong band are visible on the gel

5.9.2 Expression vector

pcDNA3 (Invitrogen see appendix), empty vector size 5.4kb, sample concentration 2ng / ul *(Fig 5.9c)* with multiple cloning sites **(for full description see appendix AP 1.13)**. Both pcDNA3vector and full length human/mouse Nav1.7 antisense transcript are double digested O/N at 37 degrees with KpnI and HindIII. Double digest conditions for HindIII and KpnI are chosen according to http://www.neb.com/nebecomm/DoubleDigestCalculator.asp for Double Digest Finder.

Digestion for 3 hours at 37 degrees in H20, Buffer NEB 2, BSA for optimal digesting conditions. To verify that the double digest was successful, both the vector and the antisense samples are loaded on a 0.9% agarosis gel and cut out under UV.
Concentrations human H.1.7 AS = 43.8ng /ul and Vec 1 = 110.5ng/ul

.

Full length cDNA human/mouse antisense transcript
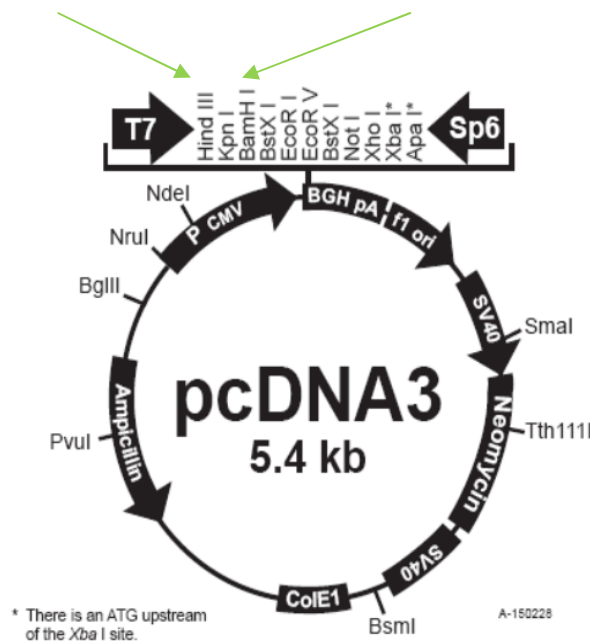
Fig 5.9c pcDNA3 Vector with MCS (multiple cloning sites) and full length human /mouse Nav1.7 antisense cDNA integrated between HindIII and KpnI. Full length Nav1.7 antisense transcript mouse: 1380bp, cDNA full length Nav1.7 antisense transcript human: 2302bp

Nav1.7 antisense transcript human/mouse is gel purified and has the final concentration after gel purification: Vec2 =131.4ng /ul; Mouse Ms1.7 AS =16.9ng/ul and Vec1 =119.3ng /ul, Vec2 =102.5ng/ul

5.9.2.2   SAP TREATMENT OF pcDNA3 ONLY

Linearized pcDNA3 Vector is treated with SAP *(see Appendix AP 1.14)*.

10ul Vector / 0.5 ul SAP incubation for 40 min at 37 degrees and 20 min for 72 degrees.

5.9.2.3   Ligation of full length NAV1.7 antisense transcript to pcDNA3 vector.

Equation to determine best vector: insert ratio for ligation.

$$\frac{\text{Vector (ng)} \quad x \quad \text{insert size (kb)}}{\text{Size of vector (kb)}} \quad x \quad 3: 1 \text{ or } 5:1 \text{ ratio}$$

Table 1: Ligation approaches human Nav1.7 antisense expression vector

Ratio	Vector (Vec2)	Insert(44ng/ul)	H20
5:1	10ng(0.76ul)	50ng(4.84ul)	Up to 17 ul
3:1	10ng(0.76ul)	30ng(2.90ul)	Up to 17 ul
1:1	10ng(0.76ul)	10ng(0.97ul)	Up to 17 ul
Plus ligase	10ng(0.76ul)	x	Up to 17ul
No ligase	10ng(0.76ul)	x	Up to 17ul
Neg control	x	x	Up to 17ul

Table 2: Ligation approaches mouse Nav1.7 antisense expression vector

Ratio	Vector (Vec2)	Insert(16.9ng/ul)	H20
5:1	10ng(0.83ul)	50ng(7.52ul)	Up to 17 ul
3:1	10ng(0.83ul)	30ng(4.51ul)	Up to 17 ul
1:1	10ng(0.83ul)	10ng(0.70ul)	Up to 17 ul
Plus ligase	10ng(0.83ul)	x	Up to 17ul
No ligase	10ng(0.83ul)	x	Up to 17ul
Neg control	x	x	Up to 17ul

Ad table 1 and 2: control reactions (1) Plus ligases was used as background control (2) No ligases determine the degree of undigested vector pcDNA3 (3) negative control with H20 instead of insert determines general contamination

- **Ligation Mix**: T4 Ligase (Fermentas), T4 ligase Buffer (Fermentas), H20. Ligation Master Mix is added, followed by 1 hour incubation at 22 degrees. At this point reactions can be stored at – 20 degrees.

5.9.2.4 Transformation of human/mouse antisense ligations into chemically competent E.coli cells

Transformations were plated out onto LB/Agar + Amp plates and incubated O/N at 37 degrees. Transformation protocol for see **XL10 – Gold ultracompetent cells.**

On the water negative control plates no colonies were visible. A few colonies appeared on the plates with "no Ligases" and "plus Ligases ". Ten single colonies were picked from positive 3:1, 5:1 plates and inoculated into 5 ml LB+Amp and incubated O/N shaking at 220 rpm at 37C. The bacterial cells were harvested by centrifugation at 5000 rpm for 10 min, and supernatant was discarded while the pellet contains the amplified expression vector. This step is followed by Miniprep and double restriction digests **(Fig 5.9.a)** with HindIII and KpnI to check for positive colonies that have inserted the full length antisense transcript into the vector.

Gel purification **(see 5.3.5)** of the positively transformed samples. As our gene of interest was already positively inserted into the vector, 2 chosen samples were re – transformed into XL-10 Gold ultracompetent cells **(Invitrogen, see 5.3.1)** and plated on LB+Amp plates and incubated O/N at 37 C. Single colonies from the LB+Amp plates were brought into a 5 ml LB +amp day culture, and let to grow shaking 250rpm for approximately 7 h at 37 C. Day cultures were then transferred into Maxiprep cultures, 500 ml LB +amp, incubated O/N, shaking at 250 rpm at 37 C and then Maxiprepped (Qiagen, high speed Maxiprep **see 5.3.4**). DNA was eluted in 1ml Elution Buffer EB and concentrations measured using Nanodrop: Human (EXPH1) = 413 ng /ul; Human (EXPH2) = 345 ng/ul; Mouse (EXPM1) = 204 ng/ul; Mouse (EXPM2) = 276.3 ng/ul

To ascertain that there were no rearrangements or deletions of the full length (A) human (B) mouse full length SCN9A antisense transcript vectors, double digest with KpnI and HindIII was performed **(Fig 5.9e).** 5 ul of each samples were loaded onto 0.9% agarosis gels.
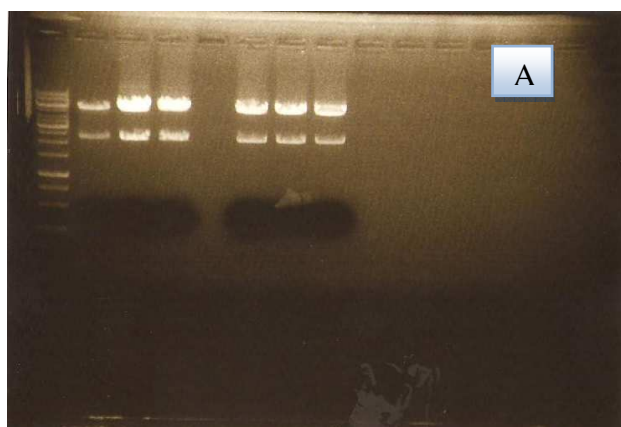
Fig 5.9e Double Digest with KpnI and HindIII after Maxiprep *to check that the expression vector constructs have positively integrated our insert of interest (A) human (B) mouse full length SCN9A antisense transcript.*

Samples that contain the full length human/mouse antisense transcript according to the right size on the analytical gel are diluted in EB to a concentration of 110ng/ul for sequencing with primers (for mouse ***(see mouse antisense primers 5.10.1.3***) and for human ***(see human antisense primer 5.10.2.3)).*** Primers are chosen and designed to give partially overlapping sequences of full length human/mouse SCN9A antisense transcript.

5.9.2.5   Sequencing - Bioinformatics

Sequencing results of each partial sequence were individually compared against reference sequence databases using the Genome UCSC (http://genome.ucsc.edu/) and NCBI BLAST (http://blast.ncbi.nlm.nih.gov/Blast.cgi) web tools. Nucleotide *blast* (Data base: Reference genomic sequences (refseq_genome), organism: mus musculus taxid: 10090 or Homo sapiens taxid: 9606) identified the sequenced inserts as full length human BC051759 and mouse AK138532 full length SCN9A antisense transcripts. Expression vectors are stored at -20C.

5.9.3   Additional vectors: pEGFP

pEGFP vector has the size of ~ 3.4kb and encodes for a red shifted variant of a wild type GFP (AP 5.9.4), GFPmut1 with an excitation maximum at 448 nm and emission maximum at 507 nm***(Fig 5.9f).*** For full information on pEGFP vector with MCS and additional features ***see Appendix AP1.15*** (or http://www.pkclab.org/PKC/vector/pEGFPN1.pdf)
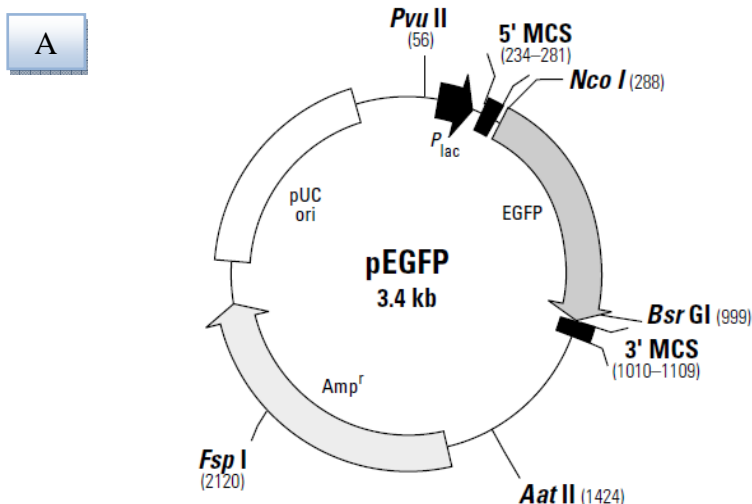
Fig 5.9f (A) EGFP vector *with and restriction map and MCS*

5.10   Primer mouse Nav1.7 sense and antisense transcript

5.10.1.1   Primer mouse Nav1.7 Antisense transcript

M1.7 AS1 FWD 5'- GAACCAGGTCTTGCTTTTCG -3', REV 5-'CCACGCTTTCCTAGAGC-3'
Size 625bp;

M1.7 AS2 FWD 5-'GGAAGGGACATCATCAGAGC-3' REV 5-'TCATTTTAATGAATCAAGCCTTA-3' size 908 bp

M1.7 AS3 FWD 5'-GATCAGGCGTAGGATTCGTC-3', REV 5'-CATAGACACTGCGTGCTGCT-3', size 624bp

M1.7 AS4 FWD 5'- GCACGACTTCTCCTGCTGC-3', REV 5'-CARAGACACTGCGTGCTGCT-3' size 879bp

5.10.1.2   Full length SCN9A antisense transcript

Name	Sequence 5'-3'	Size	Tm
MS HindII FWD	CCCAAGCTT GAGCAAGAGT AAGAAGTA	1347bp	61.4
MS KpnI REV	CGG GGTACC GCCATTATATTTCAT		

5.10.1.3   SCN9A sense - sequencing

Name	Sequence 5'- 3'	Size	Tm
Runs from	NM_018852 500 – 1504		
M1.7 RXN 1 FWD	CTCTTAGGTAAGGATCCGAAGGGG	1004 bp	69
M1.7 RXN 1 REV	GAAACCGCAAAGAAGAGCATCTTG		
Coding sequence	NM_018852 1365-2616		
M1.7 RXN 2 FWD	ATAAATGTTTCCGGAAGGACCTTG	1251 bp	68
M1.7 RXN 2REV	ACTGTGTTGGTTAGAATGCTTGCTC		
Coding sequence	NM_018852 2447-3657		
M1.7 RXN 3 FWD	GGACCCTCAGCCCTCATGCTC	1210 bp	72
M1.7 RXN 3 REV	CTTATCTCCGCAAGGGTACGGTTTG		
Runs from	NM_018852		
M1.7 RXN 4 FWD	TCCAAAAAGCCAAAGGGCTCCA	1096 bp	67
M1.7 RXN 4 REV	GCACATTTCCACTAACATTCATCAG		
Runs from	NM_018852		
M1.7 RXN 5 FWD	TGTGTTAACACCACAGATGGCTC	701 bp	69
M1.7 RXN5 REV	AAATCAAAAATGTTCCATCCCACG		
Runs from	NM_018852		
M1.7 RXN 6 FWD	GGCAAACTGACTACATGAGTTTTG	1375 bp	65
M1.7 RXN 6 REV	TGTAAACAGTGTATCAAAACCGGC		

5.10.1.4   Additional   Sequencing Primer

T7 5'- TAATACGACTCACTATAGGG-3'**, SP6** 5'-TACGATTTAGGTGACACTATAG-3'

5.10.1.5   Mouse tissue panel

Sense: M1.7 RXN 6 FWD 5'-GGCAAACTGACTACATGAGTTTTG-3',

 M1.7 RXN 6 REV 5-'TGTAAACAGTGTATCAAAACCGAAGC-3'

Antisense: M1.7 AS 1 FWD 5'- GAACCAGGTCTTGCTTTTCG,

M1.7 AS 1 REV 5'CCACGCTTTGTTCCTAGAGC-'3

Housekeeping gene HPRT 1: FWD 5'- GATGATGAACCAGGTTATGACC-3',

REV 5' –TTTCCAGTTTCACTAATGACAC-3'

5.10.2   Primer human Nav1.7 sense and antisense transcript

5.10.2. 1   Primer Human BC051759 antisense transcript: full list

H 1.7 antisense 1 FWD 5'-GGAATTCAGGCAAAGTTGGA-3', H 1.7 antisense 1 REV 5'-
CACCAACATTCAGCCATTTG-3 size 991bp

H 1.7 antisense 2 FWD 5'-GGATCACTCGGAACAGGGTA-3' , H 1.7 antisense 2 REV 5'-
CACCAACATTCAGCCATTTG-3'size 819bp

H1.7 Primer set 1 FWD 5'- CACCAGCGACAAAGAAGTCA-3', H1.7 Primer set 1 REV 5'-
AGGGAGTGACGCACAAAAC-3' size 1572

H1.7 Primer set 2 FWD 5-'GCCTCAAGTGATCCTTCTGC-3', H1.7 Primer set 2 REV 5'-
TTTTCTCACTGGGATCTGTCC-3' size 2000bp

H1.7Primer set 3 FWD 5'-GTGGGAGCGTACAGTCATCA-3', H1.7Primer set 3 REV 5'-
AGGGAGTGACGCACAAAAC-3' size 1017

5.10.2.2   Full length SCN9A antisense transcript

Name	Sequence	Size	Tm
Hm HindIII FWD	CCCAAGCTTGTCTTAGTCCTCTGAATATTTT	2302bp	58.5
Hm KpnI REV	CGGGGTACCCCAATTGATGGAGAATTTTAT		

5.10.2.3   Sequencing primer

T7 5'- TAATACGACTCACTATAGGG-3', **SP6** 5'-TACGATTTAGGTGACACTATAG-3'

BC05179XX FWD 5'-GACTTTTGGAGTAATCATGGAA-3'

5.11   Cell culture

All cell culture work (e.g. cell splitting, media preparation, transfections and coverslip
coating) are performed under a previous EtOH sterilized hood to ensure maximum sterility.
Lab coat and gloves sterilized with EtOH must be worn at all times.

5.11.1 Cell Lines

HEK 293 cells that stably express Nav1.7 were generated by stable co transfection of HEK 293 cells with an alpha subunit and a beta1 subunit of human sodium channel 1.7 (Scottish Biomedical).

HEK 293 Nav1.6 L40 cell line was generated by stable co transfection of HEK 293 cells with an alpha subunit and a beta1 subunit of human sodium channel 1.6 (Scottish Biomedical).

5.11.2 Cell culture media – MG

MEM (Sigma M5650), 2mM L- Glutamine (Sigma G7513), 10% FBS Heat inactivated (Invitrogen 2011-11), 2ug/ml Blastocydin (calbiochem 203350), 0.6mg/ml Geneticin (Invitrogen 10131-027), 10ml/L Penicillin –streptomycin (Sigma P0781). All reagents were filtered under the lamina through Stericup/Steritop filter (Millipore) to avoid contamination.

5.11.3 Cell splitting

Aspirate media and incubate with trypsin for ~2-3 minutes. Aspirate trypsin and resuspend in 10 ml of culture media MG Nav1.7 stable and wash off the cells. Transfer suspension into 15ml tubes and centrifuge 5 min at 800rpm. Aspirate supernatant and resuspend cell pellet in 10 ml MG stable cell media. Cells are split into 2ml dishes or a flask. Best transfection results are obtained with cells at around 90 per cent confluence on the day of transfection.

5.11.4 Coating

Both BD Matrigel (BD Biosciences) and DMEM (Sigma M5650) need to be permanently kept on ice. 200ul Matrigel is added to 20ml filtered DMEM without FBS (Invitrogen 2011-11). After gently mixing the reaction 300ul of the mixture is added to coverslips in a 24 well plate and incubated for 30 minutes at RT. Aspirate excessive Matrigel and replace with 500 ul cell suspension, placed onto each coated coverslip/well.

5.11.5 Transfection
5.11.5.1 Transfection of Nav1.7 stable expressing cell line for immunohistochemistry

Nav1.7 cells with an approximately 90% confluence were transfected with (1) no DNA (2) EXPH1, pcDNA3 vector containing full length human SCN9A antisense transcript **Concentration:** (EXPH1) = 413 ng /ul; According to the manufacturer's protocol, DNA was mixed with Lipofectamin in a 1:2.5 ratio.

Transfection solution was slowly and drop wise added to the Nav1.7 cells and incubated for 6 h at 37C /5% C02. After 6h the transfection solution was aspirated and replaced with MG stable cell culture medium *(see 5.11.2)*. Cells were incubated at 37C / 5 % CO2 for 24hr.

5.11.5.1.1 Immunohistochemistry

MG stable medium is firstly aspirated. Gently add ice cold methanol to each well and put well plate for 5 minutes into the -20 C freezer.

Have ice cold acetone in a glass bottle ready. Coverslips are dipped shortly into ice cold acetone and left to air dry on paper. Remaining coverslips which are not used for further analysis can be stored at -20C. Add 3% BSA blocking solution in 1x PBS for at least 45 minutes at room temperature. Aspirate off blocking solution. Prepare a 1/500 dilution of N68/6 Monoclonal mouse anti-Nav1.7 in 3% blocking solution. Add 250 ul to each coverslip and incubate for at least 1 h at room temperature. Wash three times with blocking solution. Add 1/1000 dilution of secondary antibodies in blocking solution (Invitrogen A11032 – 594 goat anti-mouse). Add 250 ul to each coverslip (except 1 one coverslip and incubation for 1 h at room temperature). Remember to include no primary antibody and no secondary antibody controls. Wash coverslips two times with blocking solution and two times with PBS. Finally add a 1/5000 dilution of DAPI/ PBS for nucleus staining. 250 ul of DAPI/PBS solution per well are added and incubated for 5 minutes at room temperature. Washing steps: three times with PBS, one time in ultra-pure sterile water. Mount cells with ProLong Gold antifade reagent and let coverslips mounted to glass slides dry on the slides overnight at 4 degrees. Coverslip edges are sealed with nail varnish before microscopy. Store slides at -20C.

5.11.5.2 Transfection of Nav1.7and Nav1.6 stable cell line for patch clamp

Cell lines stably expressing Nav1.6 or Nav.1.7*(see 5.11.1)* are split into 2ml dishes and were grown to 90% confluence for transfection with (A) no DNA as a negative control to check for any contamination of either Lipofectamine 2000 (Invitrogen), Optimem (Invitrogen 11058-021)., (B) pEGFP-N1*(see 5.9.3)*, to determine transfection efficiency and (C) EXPH1 ,expression vector pcDNA3 containing human full length Nav1.7 antisense transcript BC051759 *(see section expression vector design 5.9.1A – 5.9.2.5)* and (D) EXPH1 co transfection with pEGFP-N1 to detect transfected cells assuming that cells that take up the expression vector also take up pEGFP- N1. (E) Empty pcDNA3 vector as transcriptional control.

Vector concentration: (pEGFP-N1) =308ng/ul; (EXPH1) =413 ng/ul; (pcDNA3) = 2mg /ul.

To obtain comparable results from each transfection for approached A – E an equal amount of DNA was used for transfection of the stably expressing Nav1.6 and Nav1.7 cell lines

Highest transfection efficacy was experimentally found at a DNA: Lipo2000 ratio of 1:2.5.

Table 2 Overview of transfection approaches (patch clamp)

A. Reagent	No DNA	EGFP-N1	EXPH1	EGFP-N1+ EXPH1	pcDNA3
Lipo2000(ul)	3.125	0.625	2.5	3.125	2.5
Optimem (ul)	250	250	250	250	250
B.DNA used					
concentration	No DNA	308ng/ul	413ng/ul	308/413ng/ul	2mg/ul
in ul	No DNA	0.81	2.42	0.81/2.42	0.5
in mg	No DNA	250	1000	250/1000	1000

Add Table 2 Overview of transfection approaches: *gives a schematic overview of each performed transfection approach with reagents, concentrations, volumes and ratios used for each transfection approach. EXPH1 **(see expression vector 5.9.2)**, pcDNA3 vector that has full length antisense transcript integrated .EGFP-N1, green fluorescence protein (see 5.9.3) to evaluate transfection efficiency.*

Following transfection, cells are split to <50% confluence so that single cells can be analysed by patch clamping two days after transfection

6. Results SCN9A and its corresponding antisense transcript

6.1. Bioinformatics

By browsing the human and mouse genomes for SCN9A, several ESTs are found on the GENOME UCSC browser (http://genome.ucsc.edu/) which are partially complementary to the SCN9A gene. SCN9A encodes for a voltage gated sodium channel which is predominantly found in DRG and sympathetic ganglion neurons.

In search for the human antisense gene, several expressed sequence tags (ESTs) (BC051759, BC029452, BM905527, BE566126, BG215777, AA383040) were found which suggested a cDNA/mRNA comprised of at least 12 exons, four of which are complementary overlapping the SCN9A sense exons encoded on chromosome 2. The longest human EST is BC051759. For all ESTs, five of their exons are associated with Alu's, SINEs, and LINEs. The final exon has a polyadenylation signal and the first exon is not associated with a CpG island. For the mouse antisense gene, we identified the following antisense ESTs AK039017 (hypothalamus cDNA), AK045660 (corpora quadrigemina cDNA), AK020721 (hypothalamus cDNA), AK138511 (spinal cord) and AK138532 (spinal cord). Two of these ESTs are from the spinal cord where SCN9A is known to be expressed and suggests a cDNA comprised of 5/6 exons.

Bioinformatics comparison of the human and mouse antisense gene shows one of the exons is highly conserved between human and mouse and this maps to the final exon of the sense SCN9A gene.

To prove that the antisense gene exists and is not only an artefact, we screened for its expression in DRG neurons with mouse and human antisense specific primers. Mouse SCN9A antisense primers **(See *5.10*)** M1.7 AS 1 FWD, M1.7 AS 1 REV expected size 625bp, M1.7 AS 3 FWD 5'- , M1.7 AS 3 REV expected size 626bp. Human SCN9A antisense Primer H1.7 AS FWD 5'-GGAATTCAGGCAAAGTTGGA-'3, H1.7 AS REV 5-CACCAACATTCAGCCATTTG-'3 with expected size of 991bp. DRG RNA was freshly prepared from black 6 mice and human DRG total RNA was purchased from Clontech. These DRG RNA samples were reverse-transcribed into cDNA and used as PCR templates.

Strong and clear bands for the human and mouse Nav1.7 antisense transcript appear on the agarosis gel suggesting that the SCN9A corresponding antisense transcript is not an artefact but a real transcript that is expressed in dorsal root ganglia. To further verify that the bands

for human and mouse Nav1.7 antisense transcript were as expected, the bands were cut out, gel purified and DNA sequenced.
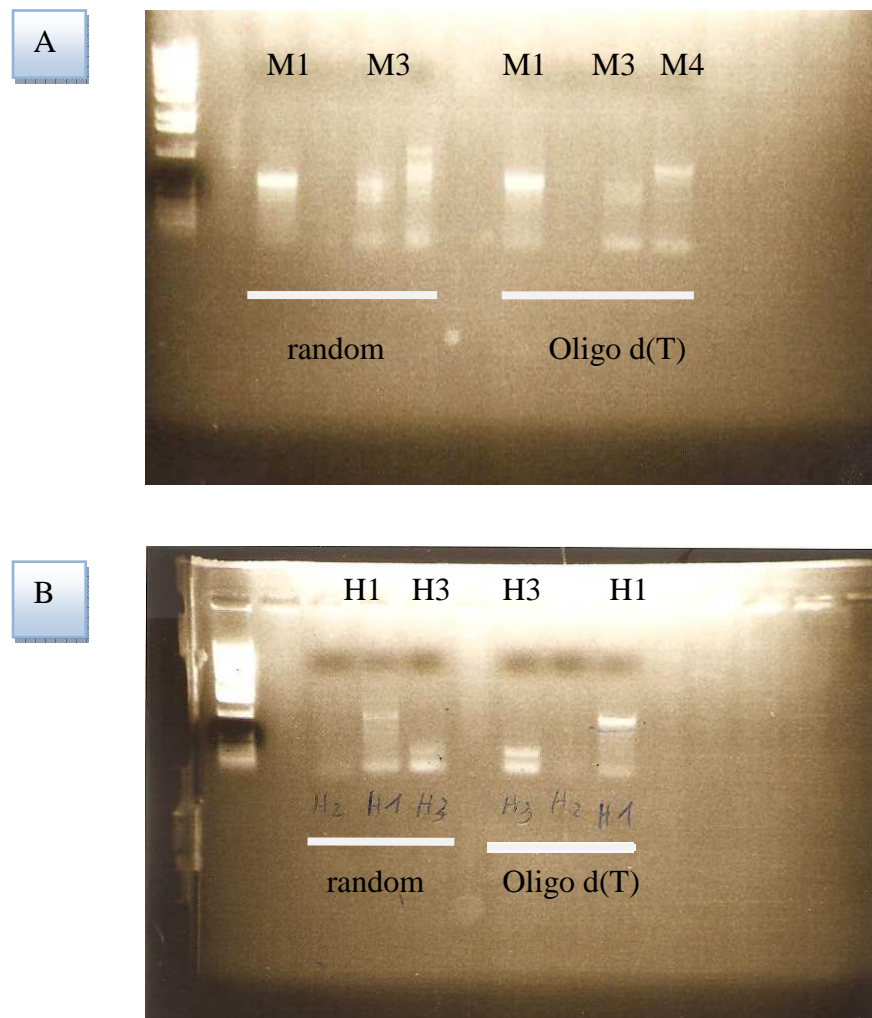
Fig6. 1(A) Clear and strong bands for M1 and M3 and (B) H1 and H3 suggest there is an antisense transcript expressed in mouse and human DRG neurons.

The primers which are used for sequencing are identical to the ones used for Phusion PCR reaction Mouse Nav1.7 AS 1 and 3, and Human Nav1.7 AS 1 and 3.
NCBI Blast (http://blast.ncbi.nlm.nih.gov/Blast.cgi) of human and mouse sequencing data against the whole genome gave a 100 per cent sequence ID of the human sequence data H1 and H3 to the human BC051759 antisense transcript and the mouse sequencing data M1 and M3 to the mouse AK138532 antisense transcript (supplemental data 2).

6.2   Mouse tissue panel

To test whether the sense and antisense transcripts are co expressed in different tissues, an RT-PCR using a mouse total RNA panel was performed. 15 different tissue specific RNA samples from the Clontech kit and one sample of freshly isolated DRG RNA were reverse-transcribed into cDNA with Superscript II and used as PCR templates with HPRT1, SCN9A sense and antisense specific primers. HPRT1 is a house keeping gene that is involved in the purine salvage pathways and was used as a reference PCR **(56)**. HPRT1 is constantly and almost equally expressed in all tissue samples tested, confirming that reverse transcription was consistent and successful across all tissues. Furthermore, sequencing results verified that our specific primers correctly amplified the SCN9A and AK138532 antisense gene in the given gels. The agarosis gels show that SCN9A is highly expressed in DRG, brain, eye, smooth muscle and spinal cord samples. These findings are identical with the prior Microarray expression pattern Data for Mouse (GNF Expression Atlas 2 Data from GNF1M Mouse Chip, GENOME USCS). Although SCN9A is mainly found in the peripheral DRG neurons, it is also weakly expressed in the CNS. The microarray data also evaluates which brain tissue particularly expresses SCN9A: Hypothalamus and weak expression in the substantia nigra and the frontal cortex. **(MICROARRAY, GENOME USCS)**

Interestingly, SCN9A antisense transcript is mainly found in the brain, spinal cord, DRG and eye samples, with highest expression in the brain and spinal cord. In contrast to the SCN9A sense gene, the antisense gene is not detectable during any developmental stage or in smooth muscle tissue. Several studies have reported an important role for Nav1.7 in cultured human smooth muscle cells such as coronary arterial, pulmonary arterial and bronchial smooth muscle cells but not freshly isolated rabbit **(58)** aortic smooth muscle cells and human pulmonary artery smooth muscles **(59).**However, in brain, DRG, eye and spinal cord tissue samples, both sense and antisense transcripts co- expression was detected. Although it is very tempting to make an assumption about the expression level of sense and antisense gene in the used tissue samples due to variation in band intensity the expression levels needs to be fully evaluated by quantitative RT- PCR and protein levels assessed by western blotting. Nevertheless, this semi-quantitative result highlights that the sense and antisense transcripts are expressed in a broadly similar tissue expression pattern.

Sense and antisense specific PCR showed a significantly different expression pattern during development stages D7, D11 and D15. While the SCN9A sense gene is expressed during D11 and D15, SCN9A antisense transcript is not amplified from the D7 to D15 samples. It has been reported that the SCN9A sense gene has different splicing variants, one of which is neonatal (57). Exon 5 is alternatively spliced in SCN9A and its neonatal splicing variant has significantly different electrophysiological properties. The exact purpose of a neonatal splicing variant is yet not fully known. However, the complete absence of antisense transcript during the developmental stage D7 to D15 gives rise to the idea that the antisense transcript might shift the splicing event in favour of one transcript rather than the other. The proposed mechanism is that expression of the antisense transcript stabiles the adult transcript, or binding masks the splicing site of the primary mRNA and therefore represses the neonatal splicing variant in favour of the adult one. The SCN9A sense primers were not specifically designed to detect a certain splice variant and unfortunately the bands appearing on the gel for the early developmental stages were not sequenced. Therefore there is no evidence that the bands on the gel are the neonatal splice variant. A different explanation for the absence of SCN9A antisense transcript in D7, D11 and D15 could be that SCN9A antisense transcript is only found in adult mice and has nothing to do with neonatal splicing variant or the antisense transcript was simply not detectable on the gel due to its low expression level.
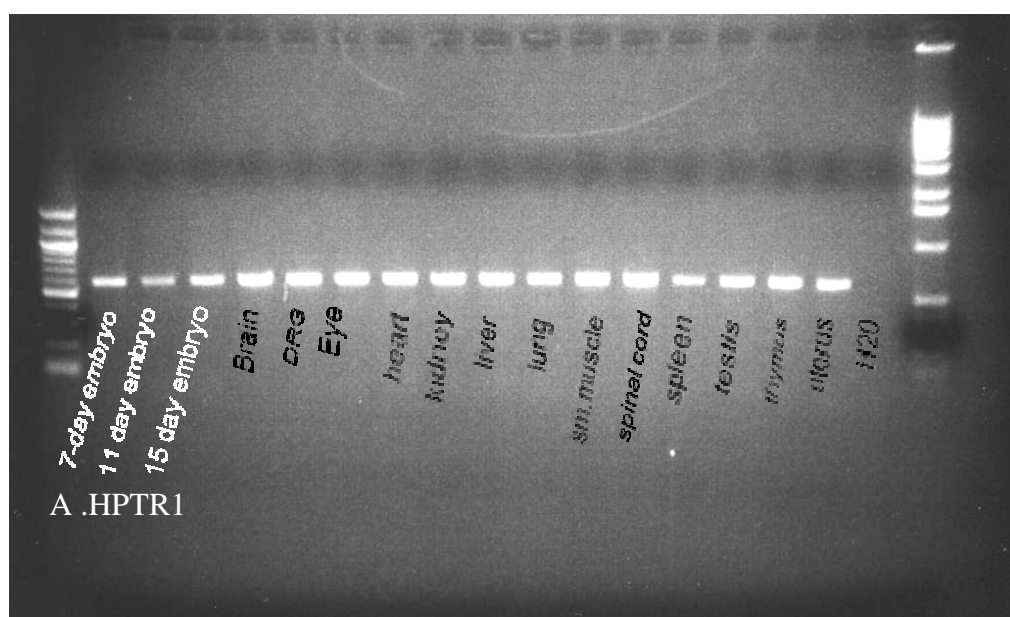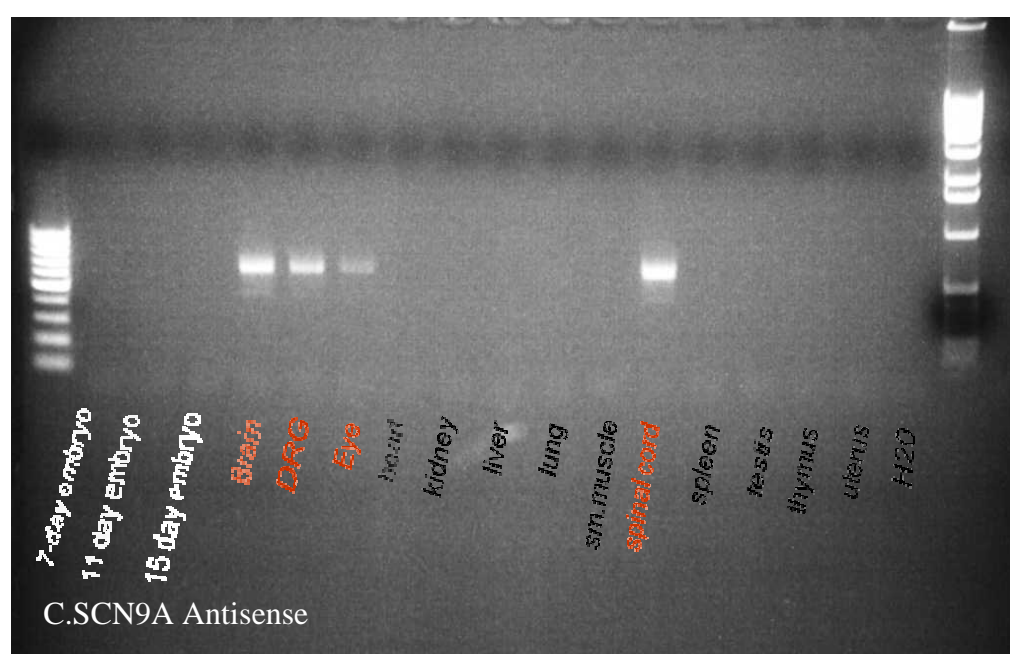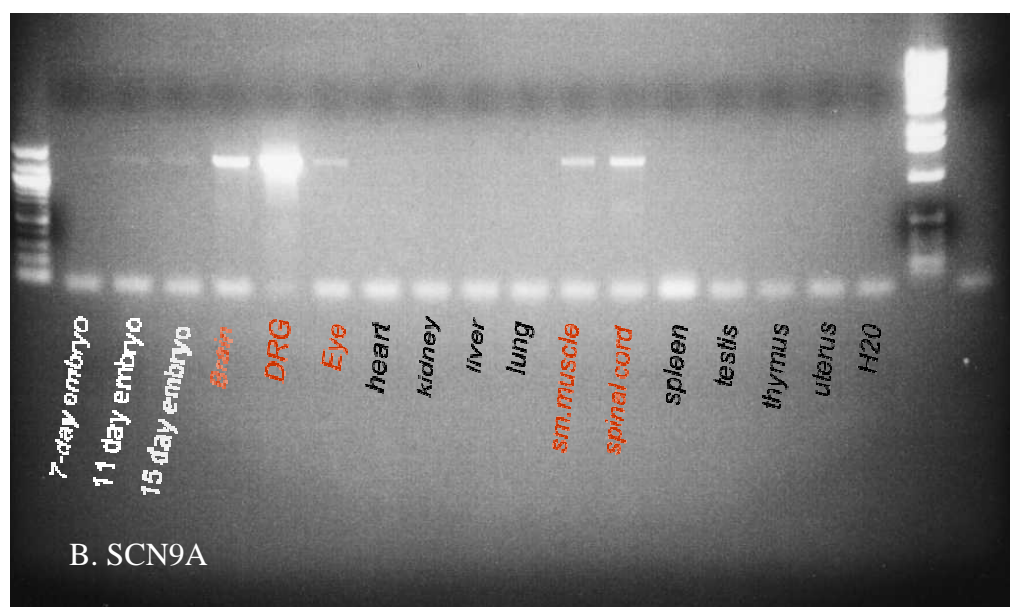
*fig X **Mouse tissue panel for (A) Housekeeping gene (B) SCN9A sense and (C) SCN9A antisense gene.** HPRT 1, a housekeeping gene, is expressed in all tissues and in all developmental stages tested .There is a spatial and temporal difference in the Nav1.7 sense and antisense transcript expression pattern. In particular the mouse Nav1.7 antisense transcript is strongly expressed in the Brain, Eye, DRG neurons and spinal cord but seems not to be expressed during the early developmental stages D-7,-11 and D-15. In comparison Nav1.7 is expressed even during early development and is also found in brain, eye and spinal cord but as to be expected mainly in DRG neuron.*

6.3   Immunohistochemistry

Transfection of Nav1.7 stable cell line with SCN9A antisense transcript

We decided to investigate the effect of overexpressing the human antisense gene in a HEK293 stable Nav1.7 cell line. The effect of overexpressing the antisense transcript in this cell line was tested by immunohistochemistry (to semi-quantatively assess SCN9A protein levels) and by patch clamping (to study the effect on Nav1.7 sodium currents).
An expression vector containing the human antisense transcript (BC051759) was cloned and transfected into the HEK293 Nav1.7 stable cells, along with an empty GFP vector to mark positively transfected cells line *(see transfection protocol 5.11.5.1).*
It is assumed that cells that take up pEGFP are also taking up EXPH1 (the antisense construct).

One day after transfection the cells were fixed with methanol and stained with an anti-Nav1.7 antibody. Figures A-C and D-F show two fields of vision in which the antisense transcript was co-expressed with a GFP expression vector. *Fig A and D* show cells positively transfected with the GFP construct (and which also are likely to express the antisense transcript). *Figs B and E* show Nav1.7 protein stained in red. *Fig C and F* show nuclei stained with DAPI. The results show that cells which express GFP and the antisense construct are still stained with the anti-Nav1.7 antibody. There is therefore no obvious effect of overexpressing the antisense transcript on Nav1.7 protein levels. However, it must be noted that this is a cell line which itself artificially overexpresses Nav1.7, and the effect on protein levels of overexpressing the antisense transcript should be tested in cells which endogenously express Nav1.7 (such as DRG neurons) and also by a more quantitative technique.
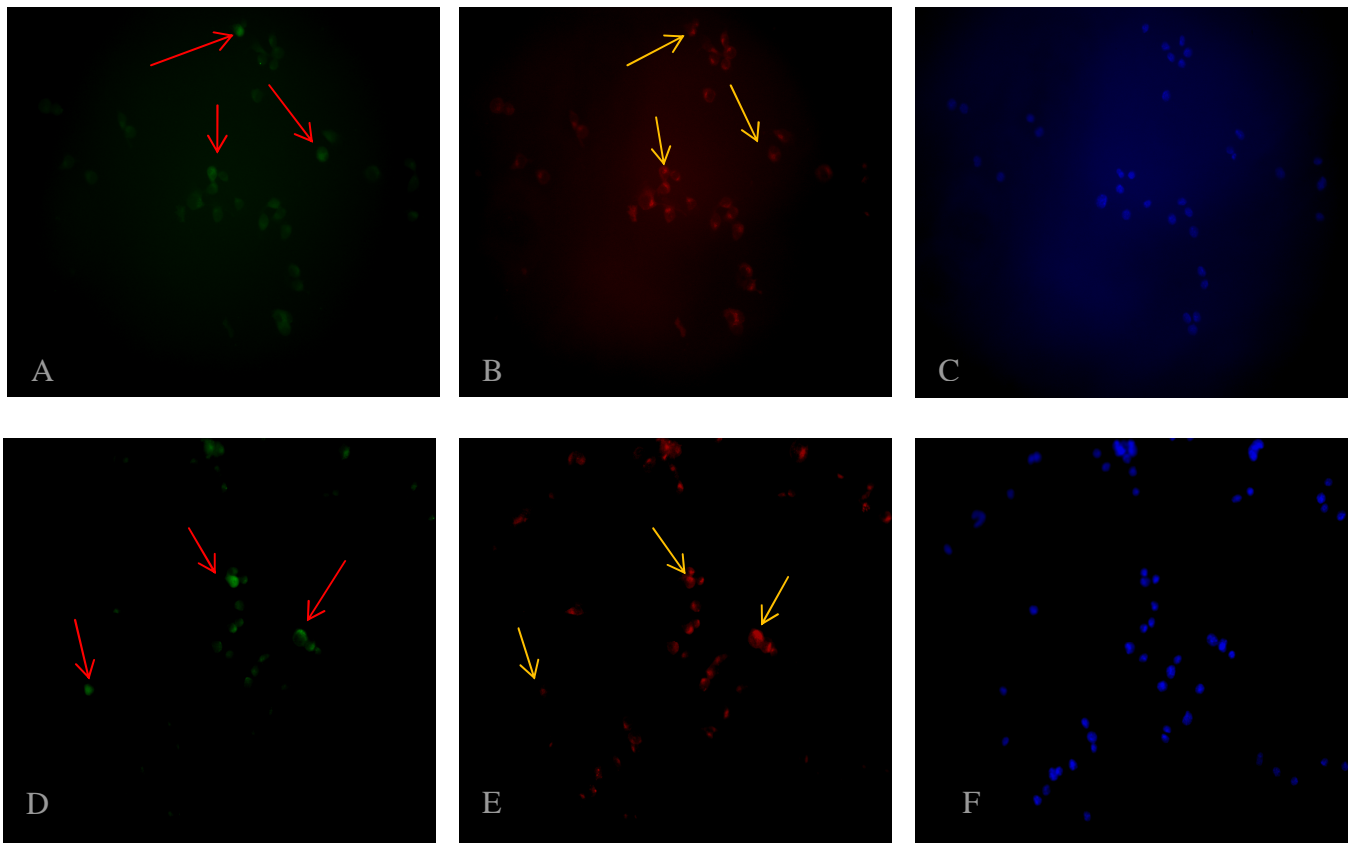
Fig A- F Immunohistochemistry. *HEK293 cells stably expressing Nav1.7 are co-transfected with a pcDNA3 vector containing SCN9A antisense transcript and a GFP vector and monitored 24h after transfection.*

A and D: *Cells positively transfected with pEGFP (and most likely the antisense construct) are shown in green.* ***B and E:*** *N68/6 monoclonal mouse anti-Nav1.7 antibody (Millipore) is used to detect the expression of Nav1.7 (in red)* ***C and F:*** *DAPI staining. DAPI (4', 6-diamidino-2-phenylindole) can pass the membrane and binds to AT rich DNA region.*

6.4 Electrophysiology

To functionally test the overexpression of the human Nav1.7 antisense transcript on sodium currents, cells stably expressing either Nav1.7 or Nav1.6 were transfected with
(1) EXPH1 and pEGFP-N1 or (2) empty pcDNA3 and pEGFP-N1. Two days after transfection the cells were patch clamped (John Linley, Post-Doc, Molecular Nociception Group, London

The results show that overexpression of the Nav1.7 antisense transcript in a cell line that stably expresses Nav1.7 results in a statistically significant reduction in the peak sodium current. In Nav1.6 stably expressing cells, overexpression of the Nav1.7 antisense construct has no effect on the sodium current. This shows that the Nav1.7 antisense transcript is specifically targeting Nav1.7.
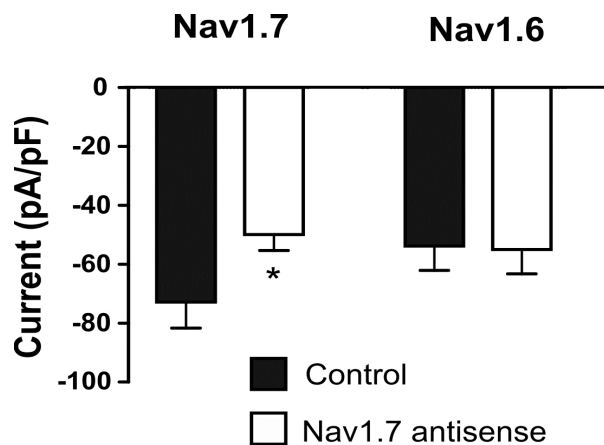
Fig *Overexpression of human Nav1.7 antisense inhibits Nav1.7 but not Nav1.6 currents.* *Whole cell voltage clamp recording from HEK cells stably expressing human Nav1.7 or human Nav1.6. Cells were transiently transfected with either pCDNA3 vector or Nav1.7 antisense and recorded from 48hrs later. Peak whole cell current (pA) was measured in response to a 10 Ms voltage step from the holding potential of -120 mV to 0 mV and normalised to cell size (pF). N = 17- 20; * indicates p<0.05 when compared to control (un-paired t-test).*

7. Discussion

Through analyses of genome browsers and using RT-PCR of dorsal root ganglia cDNA, we have identified and cloned a SCN9A natural antisense transcript (NAT) that exists in both the human and mouse genomes. The human NAT is comprised of at least 12 exons, 4 of which partially overlap SCN9A sense exons and is polyadenylated. The mouse NAT is comprised of at least 6 exons, one of which is conserved with the human NAT and overlaps the final sense SCN9A coding exon, and is also polyadenylated. The human and mouse NATs are arranged in a tail-to-tail configuration with the sense genes.

Expression analysis using RT-PCR of a commercially available mouse RNA tissue panel show that the Scn9a sense and antisense genes are expressed in broadly similar tissues (e.g. DRG, spinal cord, brain and eye). This is important because the NAT may regulate sense mRNA/protein levels in tissues in which it is co-expressed with the sense gene. It is known that antisense genes can regulate the level of sense transcript through activation of the RNAi pathway. Here, RNAi could subsequently lead to a down regulation of functional Nav1.7 channels and therefore induce a shift in neuronal excitability due to absence of functional Nav1.7 sodium channels. In RNA masking, antisense-sense transcript hybridization might mask important ribosomal binding sites leading to a reduction in translated protein. A third possible way of how the NAT might disrupt the function of the sense gene is through transcriptional collision. To further investigate this mechanism, the NAT promoter should be characterised and the temporal correlation between sense and antisense transcription should be assessed in a cell line that endogenously expresses Nav1.7. The human Nav1.7 stable cell line has the clear disadvantage that Nav1.7 is ectopically expressed in these HEK cells and differs strongly in its physiological expression that is found in DRG neurons.

By overexpressing the human NAT in a cell line that stably expresses Nav1.7, we have shown that the NAT negatively regulates the SCN9A sense mRNA leading to a significant reduction in the peak sodium current. This effect is specific to Nav1.7 as overexpressing the Nav1.7 NAT in a stable Nav1.6 cell line had no effect on peak sodium current. Whether the SCN9A

natural antisense transcript negatively regulates SCN9A by RNAi or RNA masking is not known. However, this result gives scope to further investigating the effect of overexpressing the NAT in a cell which endogenously expresses Nav1.7. Furthermore, what is particularly exciting is the possibility that downregulation of the NAT (and hence upregulation of SCN9A) might underlie different pain states. To investigate this, we plan to assess the mRNA level of the sense and antisense gene in inflammatory and neuropathic mouse pain models using quantitative RT-PCR. Furthermore, the Nav1.7 protein level will also be monitored by western blotting in these pain models. Another interesting experiment planned is to use RNA in situ hybridization to study the localization of the NATs within a primary DRG neuron so that the effect of the NAT on local protein synthesis can be explored.

As mentioned earlier *(results, 6.1 Bioinformatics)* the human and mouse antisense transcript share one highly conserved exon. It will therefore be interesting to see if transfection the of the human Nav1.7 cell line with mouse EXPM1 antisense transcript also has an effect on electrophysical properties of the human Nav1.7 voltage gated sodium channel. Overexpression of human antisense gene in a stable Nav1.7 cell line leads to a reduction of peak current. In case the conserved exon plays a central part in antisense mediated regulation in both human and mouse it is expected that we will observe the same reduction in sodium peak current as seen with the human antisense transcript. If so, his would point toward a conserved regulatory mechanism which could then be explored further.

Nav1.7 is essential in nociception and not involved in any other major cellular pathways other than pain and the olfactory pathway. Therefore the Nav1.7 voltage gated sodium channel is an attractive target for a new class of analgesic drugs. Assuming that the SCN9A natural antisense transcript regulates endogenous SCN9A, it could be possible to interfere and control this regulation and thereby control the level of functional Nav1.7 sodium channels in DRG neurons in the clinic. Similarly, it has been postulated that a natural antisense transcript to the Huntington's disease gene may have clinical applications (Ref is Chung et al 2011). So by fine tuning the level of functional Nav1.7 via antisense transcript expression it could be possible to restore normal pain thresholds even in patients suffering from inherited forms of Nav1.7 dysregulation.

References

1. Lapidot M, Pilpel Y. Genome-wide natural antisense transcription: coupling its regulation to its different regulatory mechanisms. EMBO Rep. 2006 Dec; 7(12):1216-22. Review. PubMed PMID: 17139297; PubMed Central PMCID: PMC1794690.

2. Werner A, Carlile M, Swan D. What do natural antisense transcripts regulate? RNA Biol. 2009 Jan-Mar; 6(1):43-8. Epub 2009 Jan 2. Review. PubMed PMID: 19098462.

3. Natural antisense transcript regulates gene expression in an epigenetic manner, Su WY, Xiong H, Fang JY.Biochem Biophys Res Commun. 2010 May 28; 396(2):177-81. Epub 2010 May 8. Review. PMID: 20438699

4. Lavorgna G, Dahary D, Lehner B, Sorek R, Sanderson CM, Casari G. In search of Antisense. Trends Biochem Sci. 2004 Feb; 29(2):88-94. Review. PubMed PMID: 15102435.

5. Beiter T, Reich E, Williams RW, Simon P. Antisense transcription: a critical look in both directions. Cell Mol Life Sci. 2009 Jan; 66(1):94-112. Review. PubMed PMID: 18791843

6. Werner A, Sayer JA. Naturally occurring antisense RNA: function and mechanisms of action. Curr Opin Nephrol Hypertens. 2009 Jul; 18(4):343-9. Review. PubMed PMID: 19491676.

7. Werner A, Berdal A. Natural antisense transcripts: sound or silence? Physiol Genomics. 2005 Oct 17; 23(2):125-31. Review. PubMed PMID: 16230481.

8. , Herbert A. The four Rs of RNA-directed evolution. Nat Genet. 2004 Jan; 36(1):19-25. Review. PubMed PMID: 14702037.

9. Lampert A, O'Reilly AO, Reeh P, Leffler A. Sodium channelopathies and pain. Pflugers Arch. 2010 Jul; 460(2):249-63. Epub 2010 Jan 26. Review. PubMed PMID: 20101409.

10. Larry Squire, Floyd E. Bloom, Nicholas C. Spitzer, Larry R. Squire, Darwin Berg, Floyd E. Bloom, Sascha du Lac, Anirvan Ghosh & Nicholas C. Spitzer Fundamental Neuroscience , 3rd edition , chapter

11. Waxman et al Neuroscience: channelopathies have many faces Nature 2011 Apr 14; 472(7342):173-4.

12. Dib-Hajj SD, Cummins TR, Black JA, Waxman SG. From genes to pain: Na v 1.7 and human pain disorders. Trends Neurosci. 2007 Nov; 30(11):555-63. Epub 2007 Oct 22. Review. PubMed PMID: 17950472.

13. Cummins TR, Sheets PL, Waxman SG. The roles of sodium channels in nociception: Implications for mechanisms of pain. Pain. 2007 Oct; 131(3):243-57. Epub 2007 Sep 4. Review. PubMed PMID: 17766042; PubMed Central PMCID: PMC2055547.

14. Drenth JP, Waxman SG. Mutations in sodium-channel gene SCN9A cause a spectrum of human genetic pain disorders. J Clin Invest. 2007 Dec; 117(12):3603-9. Review. PubMed PMID: 18060017; PubMed Central PMCID: PMC2096434.

15. Pain channelopathies Roman Cregg, Aliakmal Momin, Francois Rugiero, John N Wood, Jing Zhao J Physiol. 2010 June 1; 588(Pt 11): 1897–1904.   Published online 2010 February 8. doi: 10.1113/jphysiol.2010.187807 PMCID: PMC2901978

16. Cummins TR, Dib-Hajj SD, Waxman SG. Electrophysiological properties of mutant Nav1.7 sodium channels in a painful inherited neuropathy. J Neurosci. 2004 Sep22; 24(38):8232-6. PubMed PMID: 15385606.

17. Waxman et al Neuroscience: channelopathies have many faces Nature 2011 Apr 14; 472(7342):173-4.

18. Kandel James H. Schwartz Thomas M. Jessell , Fundamentals of Neural science ,4th edition , chapter 24 , The perception of pain pt 404-420

19. Isom, L. L. 2002. Beta subunits: players in neuronal hyperexcitability? Novartis Found. Symp. 241, 124–138; discussion 138–143, 226–232.

20. Cox JJ, Reimann F, Nicholas AK, Thornton G, Roberts E, Springell K, Karbani G, Jafri H, Mannan J,Raashid Y, Al-Gazali L, Hamamy H, Valente EM, Gorman S, Williams R, McHale DP, Wood JN,Gribble FM, Woods CG. An SCN9A channelopathy causes congenital inability to experience pain. Nature 2006; 444:894–898. [PubMed: 17167479]

21. The sense a comprehensive Reference , Volume 5 , Pain , section 5.07 sodium channels , John N Wood p.89-95 , Elsevier 2008

22. The Immunoglobulin Superfamily—Domains for Cell Surface Recognition
Annual Review of Immunology Vol. 6: 381-405 (Volume publication date April 1988)

DOI: 10.1146/annurev.iy.06.040188.002121

23. Catterall W.A. From ionic currents to molecular mechanisms: The structure and function of voltage-gated sodium channels (2000) Neuron, 26 (1), pp. 13-25.

24. Planells-Cases R, et al. 2000. Neuronal death and perinatal lethality in voltage-gated sodium channel alpha (II)-deficient mice. Biophys J 78:2878 –2891.

25. Wood, J. N., Boorman, J. P., Okuse, K. and Baker, M. D. (2004), Voltage-gated sodium channels and pain pathways. Journal of Neurobiology, 61: 55–71. doi: 10.1002/neu.20094

26. Lehmann-Horn F, Jurkat-Rott K, Rudel R. 2002. Periodic paralysis: understanding channelopathies. Curr Neurol Neurosci Rep 2:61– 69

27. Loss of function mutation in sodium channel Nav1.7 causes anomia ,Weiss J, Pyrski M, Jacobi E, Bufe B, Willnecker V, Schick B, Zizzari P, Gossage SJ, Greer CA, Leinders-Zufall T, Woods CG, Wood JN, Zufall F. Nature. 2011 Apr 14; 472(7342):186-90. Epub 2011 Mar PMID:21441906

28. Pain as a Channelopathy Raouf R, Quick K, Wood JN. J Clin Invest. 2010 Nov 1; 120(11):3745-52. doi: 10.1172/JCI43158. Epub 2010 Nov 1. Review.

29. Dib-Hajj SD, Binshtok AM, Cummins TR, Jarvis MF, Samad T, Zimmermann K. Voltage-gated sodium channels in pain states: role in pathophysiology and targets for treatment. Brain Res Rev. 2009 Apr; 60(1):65-83. Epub 2008 Dec 25. Review. PubMed PMID: 19150627.

30. Dib-Hajj SD, Cummins TR, Black JA, Waxman SG. Sodium channels in normal and pathological pain. Annu Rev Neurosci. 2010; 33:325-47. Review. PubMed PMID: 20367448

31. Nassar MA, Stirling LC, Forlani G, Baker MD, Matthews EA, et al. 2004. Nociceptor-specific gene deletion reveals a major role for Nav1.7 (PN1) in acute and inflammatory pain. Proc. Natl. Acad. Sci. USA 101:12706–11

32. Nassar MA, Levato A, Stirling C,Wood JN. 2005. Neuropathic pain develops normally in mice lacking both Nav1.7 and Nav1.8. Mol. Pain 1:24

33. Nassar MA, Baker MD, Levato A, Ingram R, Mallucci G, et al. 2006. Nerve injury induces robust allodynia and ectopic discharges in Nav1.3 null mutant mice. Mol. Pain 2:33

34. Fischer TZ, Waxman SG. Familial pain syndromes from mutations of the Nav1.7

sodium channel. Ann N Y Acad Sci. 2010 Jan; 1184:196-207. Review. PubMed PMID: 20146699

35. Marban, E., Yamagishi, T. & Tomaselli, G.F. Structure and function of voltage-gated sodium channels. J Physiol 508 (Pt 3), 647-57 (1998).

36. Klugbauer, N., Lacinova, L., Flockerzi, V. & Hofmann, F. Structure and functional expression of a new member of the tetrodotoxin-sensitive voltage-activated sodium channel family from human neuroendocrine cells. Embo J 14, 1084-90 (1995).

37. Herzog, R.I., Cummins, T.R., Ghassemi, F., Dib-Hajj, S.D. & Waxman, S.G. Distinct repriming and closed-state inactivation kinetics of Nav1.6 and Nav1.7 sodium channels in mouse spinal sensory neurons. J Physiol 551, 741-50 (2003).

38. Wulff BE, Sakurai M, Nishikura K. Elucidating the inosinome: global approaches to adenosine-to-inosine RNA editing. Nat Rev Genet. 2011 Feb; 12(2):81-5. Epub 2010 Dec 21. PubMed PMID: 21173775; PubMed Central PMCID: PMC3075016.

39. Zinshteyn B, Nishikura K. Adenosine-to-inosine RNA editing. Wiley Interdiscip Rev Syst Biol Med. 2009 Sep-Oct;1(2):202-9. Review. PubMed PMID: 20835992; PubMedCentral PMCID: PMC2946787

40. Nishikura K. Editor meets silencer: crosstalk between RNA editing and RNA Interference. Nat Rev Mol Cell Biol. 2006 Dec;7(12):919-31. Review. PubMed PMID: 17139332; PubMed Central PMCID: PMC2953463.

41. Athanasiadis A, Rich A, Maas S. Widespread A-to-I RNA editing of Alu-containing mRNAs in the human transcriptome. PLoS Biol. 2004 Dec;2(12):e391. Epub 2004 Nov 9. PubMed PMID: 15534692; PubMed Central PMCID: PMC526178.

42. Maas S, Kawahara Y, Tamburro KM, Nishikura K. A-to-I RNA editing and human disease. RNA Biol. 2006 Jan-Mar; 3(1):1-9. Epub 2006 Jan 12. Review. PubMed PMID: 17114938; PubMed Central PMCID: PMC2947206.

43. Abrahamsen B, Zhao J, Asante CO, Cendan CM, Marsh S, Martinez-Barbera JP,Nassar MA, Dickenson AH, Wood JN. The cell and molecular basis of mechanical,cold, and inflammatory pain. Science. 2008 Aug 1; 321(5889):702-5. PubMed PMID: 18669863.

44. Regulatory roles of natural antisense transcripts .Mohammad Ali Faghihi, Claes Wahlestedt Nat Rev Mol Cell Biol. Author manuscript; available in PMC 2010 April 7. Published in final edited form as: Nat Rev Mol Cell Biol. 2009 September; 10 (9):

637–643. Published online 2009 July 29. doi: 10.1038/nrm2738 PMCID: PMC2850559

45. Faghihi MA, Zhang M, Huang J, Modarresi F, Van der Brug MP, Nalls MA, Cookson MR, St-Laurent G 3rd, Wahlestedt C. Evidence for natural antisense transcript-mediated inhibition of microRNA function. Genome Biol. 2010; 11(5):R56.Epub 2010 May 27. PubMed PMID: 20507594; PubMed Central PMCID: PMC2898074.

46. Uchida T, Rossignol F, Matthay MA, Mounier R, Couette S, Clottes E, Clerici C.Prolonged hypoxia differentially regulates hypoxia-inducible factor (HIF)-1alpha and HIF-2alpha expression in lung epithelial cells: implication of natural Antisense HIF-1alpha. J Biol Chem. 2004 Apr 9; 279(15):14871-8. Epub 2004 Jan 26. PubMed PMID: 14744852.

47. Osato N, Suzuki Y, Ikeo K, Gojobori T. Transcriptional interferences in cis-natural antisense transcripts of humans and mice. Genetics. 2007Jun; 176(2):1299-306. Epub 2007 Apr 3. PubMed PMID: 17409075; PubMed Central PMCID: PMC1894591.

48. Farnebo M. Wrap53, a novel regulator of p53. Cell Cycle. 2009 Aug; 8(15):2343-6. Epub 2009 Aug 8. PubMed PMID: 19571673.

49. Payer B, Lee JT. X chromosome dosage compensation: how mammals keep the balance. Annu Rev Genet. 2008; 42:733-72. Review. PubMed PMID: 18729722.

50. Lee JT, Davidow LS, Warshawsky D. Tsix, a gene antisense to Xist at the X-inactivation centre. Nat Genet. 1999 Apr; 21(4):400-4. PubMed PMID: 10192391.

51. Zhou H, Hu H, Lai M. Non-coding RNAs and their epigenetic regulatory mechanisms. Biol Cell. 2010 Dec; 102(12):645-55. Review. PubMed PMID: 21077844

52. Chen, Z., Place, R.F., Jia, Z.J., Pookot, D., Dahiya, R. and Li, L.C. (2008) Antitumor effect of dsRNA-induced p21 (WAF1/CIP1) gene activation in human bladder cancer cells. Mol. Cancer Ther. 7, 698-703

53. Herbert A. The four Rs of RNA-directed evolution. Nat Genet. 2004Jan; 36(1):19-25. Review. PubMed PMID: 14702037.

54. Nav1.9 Channel Contributes to Mechanical and Heat Pain Hypersensitivity Induced by Subacute and Chronic Inflammation Stéphane Lolignier, Muriel Amsalem, François Maingret, Françoise Padilla, Mélanie Gabriac, Eric Chapuy, Alain Eschalier, Patrick Delmas, Jérôme Busserolle PLoS One. 2011; 6(8): e23083.   Published online 2011 August 12. doi: 10.1371/journal.pone.0023083 PMCID: PMC3155549

55. Wutz A, Gribnau J. X inactivation Xplained. Curr Opin Genet Dev. 2007 Oct; 17(5):387-93. Epub 2007 Sep 14. Review. PubMed PMID: 17869504.

56. M Pearce*, C Jurinke, and P Oeth. Reference gene selection for gene expression studies. Sequenome

57. Raymond CK, Castle J, Garrett-Engele P, Armour CD, Kan Z, Tsinoremas N, Johnson JM. Expression of alternatively spliced sodium channel alpha-subunit genes. Unique splicing patterns are observed in dorsal root ganglia. J Biol Chem. 2004 Oct 29; 279(44):46234-41. Epub 2004 Aug 9. PubMed PMID: 15302875.

58. Meguro K, Iida H, Takano H, Morita T, Sata M, Nagai R, Nakajima T. Function and role of voltage-gated sodium channel NaV1.7 expressed in aortic smooth muscle cells. Am J Physiol Heart Circ Physiol. 2009 Jan; 296(1):H211-9. Epub 2008 Oct PubMed PMID: 18978189.

59. Platoshyn O, Remillard CV, Fantozzi I, Sison T, Yuan JX. Identification of functional voltage-gated Na(+) channels in cultured human pulmonary artery smooth muscle cells. Pflugers Arch. 2005 Nov; 451(2):380-7. Epub 2005 Jul 29. PubMed PMID: 16052353; PubMed Central PMCID: PMC1351366.

60. Dar R., Ariely D., Frenk H.The effect of past-injury on pain threshold and tolerance(1995) Pain, 60 (2), pp. 189-193.

61. Dichgans M, Freilinger T, Eckstein G, Babini E, Lorenz-Depiereux B, Biskup S, Ferrari MD, Herzog J, van den Maagdenberg AM, Pusch M, Strom TM. Mutation in the neuronal voltage-gated sodium channel SCN1A in familial hemiplegic migraine.Lancet. 2005 Jul 30-Aug 5; 366(9483):371-7. PubMed PMID: 16054936.

62. Fertleman CR, Baker MD, Parker KA, Moffatt S, Elmslie FV, Abrahamsen B, Ostman J, Klugbauer N, Wood JN, Gardiner RM, Rees M. SCN9A mutations in paroxysma lextreme pain disorder: allelic variants underlie distinct channel defects and phenotypes. Neuron. 2006 Dec 7; 52(5):767-74. PubMed PMID: 17145499.

63. Priest BT, Murphy BA, Lindia JA, Diaz C, Abbadie C, Ritter AM, Liberator P,Iyer LM, Kash SF, Kohler MG, Kaczorowski GJ, MacIntyre DE, Martin WJ.Contribution of the tetrodotoxin-resistant voltage-gated sodium channel NaV1.9 tosensory transmission and nociceptive behavior. Proc Natl Acad Sci U S A. 2005 Jun28; 102(26):9382-7. Epub 2005 Jun 17. PubMed PMID: 15964986; PubMed Central PMCID: PMC1166597.

64. Akopian AN, Souslova V, England S, Okuse K, Ogata N, Ure J, Smith A, Kerr BJ, McMahon SB, Boyce S, Hill R, Stanfa LC, Dickenson AH, Wood JN. The tetrodotoxin-resistant sodium channel SNS has a specialized function in pain pathways. Nat Neurosci. 1999 Jun; 2(6):541-8. PubMed PMID: 10448219.

65. Wilde AA, Brugada R. Phenotypical manifestations of mutations in the genesencoding subunits of the cardiac sodium channel. Circ Res. 2011 Apr 1;108(7):884-97. Review. PubMed PMID: 21454796.

66. Levin SI, Khaliq ZM, Aman TK, Grieco TM, Kearney JA, Raman IM, Meisler MH.Impaired motor function in mice with cell-specific knockout of sodium channel Scn8a (NaV1.6) in cerebellar purkinje neurons and granule cells. J Neurophysiol. 2006 Aug;96(2):785-93. Epub 2006 May 10. PubMed PMID: 16687615

Weblinks and Bioinformatic databases: Overview

- International Association for the Study of Pain: IASP Taxomy

  http://www.iasp-pain.org

- Fantom mouse consortium , full mouse antisense clone description

  http://www.dnaform.jp/products/fantom/pd f/FANTOM-PX-PY-PZ.pdf

- RestrictionMapper http://www.restrictionmapper.org/

- Double Digest Finder http://www.neb.com/nebecomm/DoubleDigestCalculator.asp

- Genome UCSC http://genome.ucsc.edu

- NCBI Blast http://blast.ncbi.nlm.nih.gov/Blast.cgi

- For full information on pEGFP vector with MCS

  http://www.pkclab.org/PKC/vector/pEGFPN1.pdf

SUPPLEMENTAL DATA 1 -<u>SCN9A protein structure</u>

Primary amino acid sequence (5N+11RS)

```
                 10        20        30        40        50        60
./wwwt MAMLPPPGPQSFVHFTKQSLALIEQRIAERKSKEPKEEKKDDDEEAPKPSSDLEAGKQLP

                 70        80        90       100       110       120
./wwwt FIYGDIPPGMVSEPLEDLDPYYADKKTFIVLNKGKTIFRFNATPALYMLSPFSPLRRISI

                130       140       150       160       170       180
./wwwt KILVHSLFSMLIMCTILTNCIFMTMNNPPDWTKNVEYTFTGIYTFESLVKILARGFCVGE

                190       200       210       220       230       240
./wwwt FTFLRDPWNWLDFVVIVFAYLTEFVNLGNVSALRTFRVLRALKTISVIPGLKTIVGALIQ

                250       260       270       280       290       300
./wwwt SVKKLSDVMILTVFCLSVFALIGLQLFMGNLKHKCFRNSLENNETLESIMNTLESEEDFR

                310       320       330       340       350       360
./wwwt KYFYYLEGSKDALLCGFSTDSGQCPEGYTCVKIGRNPDYGYTSFDTFSWAFLALFRLMTQ

                370       380       390       400       410       420
./wwwt DYWENLYQQTLRAAGKTYMIFFVVVIFLGSFYLINLILAVVAMAYEEQNQANIEEAKQKE

                430       440       450       460       470       480
./wwwt LEFQQMLDRLKKEQEEAEAIAAAAAEYTSIRRSRIMGLSESSSETSKLSSKSAKERRNRR

                490       500       510       520       530       540
./wwwt KKKNQKKLSSGEEKGDAEKLSKSESEDSIRRKSFHLGVEGHRRAHEKRLSTPNQSPLSIR

                550       560       570       580       590       600
./wwwt GSLFSARRSSRTSLFSFKGRGRDIGSETEFADDEHSIFGDNESRRGSLFVPHRPQERRSS

                610       620       630       640       650       660
./wwwt NISQASRSPPMLPVNGKMHSAVDCNGVVSLVDGRSALMLPNGQLLPE//GTTNQIHKKRRCS

                670       680       690       700       710       720
./wwwt SYLLSEDMLNDPNLRQRAMSRASILTNTVEELEESRQKCPPWWYRFAHKFLIWNCSPYWI

                730       740       750       760       770       780
./wwwt KFKKCIYFIVMDPFVDLAITICIVLNTLFMAMEHHPMTEEFKNVLAIGNLVFTGIFAAEM

                790       800       810       820       830       840
./wwwt VLKLIAMDPYEYFQVGWNIFDSLIVTLSLVELFLADVEGLSVLRSFRLLRVFKLAKSWPT

                850       860       870       880       890       900
./wwwt LNMLIKIIGNSVGALGNLTLVLAIIVFIFAVVGMQLFGKSYKECVCKINDDCTLPRWHMN

                910       920       930       940       950       960
./wwwt DFFHSFLIVFRVLCGEWIETMWDCMEVAGQAMCLIVYMMVMVIGNLVVLNLFLALLLSSF

                970       980       990      1000      1010      1020
./wwwt SSDNLTAIEEDPDANNLQIAVTRIKKGINYVKQTLREFILKAFSKKPKISREIRQAEDLN

               1030      1040      1050      1060      1070      1080
```

```
./wwwt  TKKENYISNHTLAEMSKGHNFLKEKDKISGFGSSVDKHLMEDSDGQSFIHNPSLTVTVPI

              1090      1100      1110      1120      1130      1140
./wwwt  APGESDLENMNAEELSSDSDSEYSKVRLNRSSSSECSTVDNPLPGEGEEAEAEPMNSDEP

              1150      1160      1170      1180      1190      1200
./wwwt  EACFTDGCVRRFSCCQVNIESGKGKIWWNIRKTCYKIVEHSWFESFIVLMILLSSGALAF

              1210      1220      1230      1240      1250      1260
./wwwt  EDIYIERKKTIKIILEYADKIFTYIFILEMLLKWIAYGYKTYFTNAWCWLDFLIVDVSLV

              1270      1280      1290      1300      1310      1320
./wwwt  TLVANTLGYSDLGPIKSLRTLRALRPLRALSRFEGMRVVVNALIGAIPSIMNVLLVCLIF

              1330      1340      1350      1360      1370      1380
./wwwt  WLIFSIMGVNLFAGKFYECINTTDGSRFPASQVPNRSECFALMNVSQNVRWKNLKVNFDN

              1390      1400      1410      1420      1430      1440
./wwwt  VGLGYLSLLQVATFKGWTIIMYAAVDSVNVDKQPKYEYSLYMYIYFVVFIIFGSFFTLNL

              1450      1460      1470      1480      1490      1500
./wwwt  FIGVIIDNFNQQKKKLGGQDIFMTEEQKKYYNAMKKLGSKKPQKPIPRPGNKIQGCIFDL

              1510      1520      1530      1540      1550      1560
./wwwt  VTNQAFDISIMVLICLNMVTMMVEKEGQSQHMTEVLYWINVVFIILFTGECVLKLISLRH

              1570      1580      1590      1600      1610      1620
./wwwt  YYFTVGWNIFDFVVVIISIVGMFLADLIETYFVSPTLFRVIRLARIGRILRLVKGAKGIR

              1630      1640      1650      1660      1670      1680
./wwwt  TLLFALMMSLPALFNIGLLLFLVMFIYAIFGMSNFAYVKKEDGINDMFNFETFGNSMICL

              1690      1700      1710      1720      1730      1740
./wwwt  FQITTSAGWDGLLAPILNSKPPDCDPKKVHPGSSVEGDCGNPSVGIFYFVSYIIISFLVV

              1750      1760      1770      1780      1790      1800
./wwwt  VNMYIAVILENFSVATEESTEPLSEDDFEMFYEVWEKFDPDATQFIEFSKLSDFAAALDP

              1810      1820      1830      1840      1850      1860
./wwwt  PLLIAKPNKVQLIAMDLPMVSGDRIHCLDILFAFTKRVLGESGEMDSLRSQMEERFMSAN

              1870      1880      1890      1900      1910      1920
./wwwt  PSKVSYEPITTTLKRKQEDVSATVIQRAYRRYRLRQNVKNISSIYIKDGDRDDDLLNKKD

              1930      1940      1950      1960      1970
./wwwt  MAFDNVNENSSPEKTDATSSTTSPPSYDSVTKPDKEKYEQDRTEKEDKGKDSKESKK
```

Ion selectivity pore (PAPER) [1]

A re-entrant loop between helices S5 and S6 is embedded into the transmembrane region of the channel to form the narrow, ion-selective filter at the extracellular end of the pore.

In ion trans I: 356-365

In ion trans II: 911-920

In ion trans III: 1390-1399

In ion trans IV: 1682-1691

Transmembrane regions (Klugbauer)

Sodium Ion transport associated domain (SMART)

969-1191

Coiled coil region

402-449

IQ

1877-1899

Mutations

pedigree 44324   S459X

pedigree 22310   W897X

pedigree 21706   I767X

SNPs

rs12478318	G/T	M➔L
rs4369876	A/C	V➔L
rs6746030	A/G	R➔W
rs3750904	C/T	D➔G

Splice variants

Alternative coding exon 5:

YLTEFVNLGNVSALRTFRVLRALKTISVIP

YVTEFVDLGNVSALRTFRVLRALKTISVIP

For SCN8A it is said that this sequence encodes parts of transmembrane segments S3 and S4 within domain I [2,3].

Extension of coding exon 11 at //:

VIIDKATSDDS

For SCN8A it is said that this encodes a portion of the cytoplasmic loop between domains I and II [4].

IFM motif

In italics is the IFM motif. The sequence contains the IFM motif and the charged residues in the domain III-IV linker identified to be critical for the fast inactivation kinetics of the rat brain II channel [5].

Tetrodotoxin amino acid

Highlighted in black is Y362 which can be mutated to Serine to make the channel tetrodotoxin-resistant [6].

1. Marban, E., Yamagishi, T. & Tomaselli, G.F. Structure and function of voltage-gated sodium channels. *J Physiol* **508 (Pt 3)**, 647-57 (1998).
2. Plummer, N.W., McBurney, M.W. & Meisler, M.H. Alternative splicing of the sodium channel SCN8A predicts a truncated two-domain protein in fetal brain and non-neuronal cells. *J Biol Chem* **272**, 24008-15 (1997).
3. Plummer, N.W. et al. Exon organization, coding sequence, physical mapping, and polymorphic intragenic markers for the human neuronal sodium channel gene SCN8A. *Genomics* **54**, 287-96 (1998).
4. Dietrich, P.S. et al. Functional analysis of a voltage-gated sodium channel and its splice variant from rat dorsal root ganglia. *J Neurochem* **70**, 2262-72 (1998).
5. Klugbauer, N., Lacinova, L., Flockerzi, V. & Hofmann, F. Structure and functional expression of a new member of the tetrodotoxin-sensitive voltage-activated sodium channel family from human neuroendocrine cells. *Embo J* **14**, 1084-90 (1995).

6.   Herzog, R.I., Cummins, T.R., Ghassemi, F., Dib-Hajj, S.D. & Waxman, S.G. Distinct repriming and closed-state inactivation kinetics of Nav1.6 and Nav1.7 sodium channels in mouse spinal sensory neurons. *J Physiol* **551**, 741-50 (2003).

Supplemental data 2 – Full length antisense, cDNA sequence Mouse

Sequence: AK 138532

```
   1 gagcaagagt aagaagtatt ggcagcagca agcaggcggg caggctgaga tcttgcatgg

  61 aaatcatgaa ccaggtcttg cttttcgttt ttgaaacgtt ttggaaggag agttatgaat

 121 agcccagaaa taggtctcat tttgtgggta ggaagaatga ccagaagcat gaaagctaaa

 181 tctcctggca agtgcagggg acctctcttg gagtgtgcag taaacccgag gggacgactt

 241 ctcctgctgt caactcctga accatcacat ctggagtgaa ggaaggggct ggtgaagcct

 301 tgtaataaat gcaaaggatg ctgctgagag ctttggtctg cctttaactc attgtggcaa

 361 agttggacat cccaaagatg gcgtagatga acatgacgag gaaaagcagg aggccgatgt

 421 tgaacagcgc aggaagggac atcatcagag caaagagcag cgtgcggatc cccttggcgc

 481 ctttgatcag gcgtaggatt cgtccaatcc tggccaggcg aatgactcgg aacaggatgc

 541 tactcccagt cttcactgag aaactgctct agccagtgaa cgacagtgaa tgaagaaatg

 601 cctggctgct cgagacaccg agagtgacag ctgcgtgctc agctcaggag gacgttcata

 661 tccttcttca aggctctagg aacaaagcgt ggtgatgaca ggaagacagt aagagcccag

 721 gacataggga tgggagctat gaagctctgt gctgtaccaa ggacacaatc aatgtaatcg

 781 cggcaccata acagaggtca gcagtgggtt cgtgcaatac tgagcgggtc agcattcatt

 841 cattcatata cagagagggc ccatgcagcc acatcttctc tgctgaatta tgagctaccg

 901 atggattgtg ggagaaacaa acattctctt cagccttggg cccacttctg agttcactag

 961 gttaaacttc ttcgatgttg gcctggttct gttcctcgta cgccatggct accacagcca

1021 ggatcaagtt tatcaggtaa aaggatccca gaaatatcac cacgacaaag aaaatcatgt

1081 aggttttgcc agcagcacgc agtgtctatg gggagcaaaa aagagacatg attattttag

1141 taatacaaaa atttcactaa ggtttttatt gcagctagta tataatgaat gtgcaaacca

1201 gatatttttg tataattttg ttgtagaaag ataaataaag ataatatctt tgaggaaaat

1261 cagtattaaa caaacttttt aatataaaag atacagcatt gttatatgta cattaaggct

1321 tgattcttca ttaaaatgaa atataatggc
```

Human full length antisense , cDNA sequence
Sequence = BC051759

```
gtcttagtcc tctgaatatt ttttctttgt tcagaacctg agaaagatga atgaaattta
      61 gtgtttccca tccccgagag acacccagca tccacaactt cacactctga tgccattgtg
     121 tatttatgca agaaatacca taactaagat gaggtctcgc tatgttgcct aggctagtct
     181 tgaactcctg gcctcaagtg atccttctgc ctcagcatcg ggagtcactg ggattaaagg
     241 catgagccac catgctcagg aacttgacat catcagacag taaatcaaga ggtactgaca
     301 actgagactg agtgatggtc cctgcctagg atttggaatc tttgcatgaa atagggactc
     361 tagccaccag cgacaaagaa gtcagggaga ctgcggtctc taggaagcac ttccaggaaa
     421 caggaattca ggcaaagttg gacattccaa agatggcgta gatgaacatg accaggaaga
     481 gcaggaggcc gatgttaaac aacgcaggaa gggacatcat caaagcaaag agcagcgtgc
     541 ggatccccctt tgctcctttg actagacgta ggattcggcc aatcctggca agacggatca
     601 ctcggaacag ggtaacagag atctctggag gtgaaacatt gctctgaact ggcattgatt
     661 ctagcccagc tcttgtagac caattaccaa cttgtccatc tccctccagt gcctggaact
     721 ggacctggca cacaggcctc tggctcatcg gaattcatag gttcagcctc tgcttcttct
     781 ccttctccag gcaaagggtt atcaactgtg ctgcactctg aggagcttga ccggtttaat
     841 ctctagaaag gaattcacca ccccaccagc acgcggaaca caatcaggaa ggagtggaag
     901 aagtcgttca tgtgccaccg tgggagcgta cagtcatcat tgatcttgca gacacattct
     961 ttgtagctct taccaaagag ctgcatgccg accacagcaa aaatgaagac gatgatggcc
    1021 aacactaagc ctttagacta aaaagaaaac aaatattaca taccctgaat ctgtgctgaa
    1081 accacaaagg agagcatctt tggatccttc caagtaataa aaatattctg ttgaagaaga
    1141 atttgaacag ttataacatc acagacttta atctgtgatt gtgataaagg aggtcaaatt
    1201 aaaaaatctg attattggga gactttggga gtaatcatgg aagaaagact atgaaatcag
    1261 atattcttgg atttgaatgt tgcttctatc ccttcttaac ttaaatccat gggcattcat
    1321 tatcatcagt gcctaacctg gcagaaccac agtctacaca taatctggca tctgtctttt
    1381 ccatgctggc taccaaatgg ctgaatgttg gtggagaaac tctcacaacc aagtgaatgg
    1441 ttatatttta atttcgctct tgttgcccag tctggagtgc aatggcacga tctcggctca
    1501 ccgcaacctc tgcctcccga gttcaagcga ttctcctgcc tcagcctcct gagtagctgg
    1561 aattacaggc acccaccacc atgcccggct aatttttgt atttttagta gagacggggt
    1621 ttctttttt ttcttctttt tttgtattat tttttagcaa aaaaaaaaa aaaatacatg
    1681 aagcaattcc agaaagcgat gaattaaatt aaatttgatt aaaggctgtc tgtgtacata
    1741 gagaattgca atctaacttc atatgtaaac aaattgcatt ctaatctatt agtatattct
    1801 tgtaacaagt agctgtctca gccaatcaca gcagctgagc ttcagccaac cacagcctgc
    1861 tgatttatca gacaatgtcc acataaggca aatgtcaagc tataagcaat caagctgttt
    1921 ttgtgcgtca ctccctttt ctgtctataa atactcctgc tcatgttgct gagttgagct
    1981 ctccgaactt ctcttggttc tgagtgctgc ctaaatcatt attattatta tcttatttca
    2041 gcaataaata ctatttcatt gctgaaataa gctgctaaat ttaatttgtt gaaatttttt
    2101 cttttaacaa aggttaagaa aaccattcac agtataaact cagaaatagg agcaagactc
    2161 agaataaaag gacagatccc agtgagaaaa cttaagttta aataagtgtg gtaaaataat
    2221 ctacaatatt aaatgtaagt tactcatcag atatattaat tttacagcat ataaattaag
    2281 aaataaaatt ctccatcaat tgg
```

AP1.1 1 kb DNA Ladder, Invitrogen
http://products.invitrogen.com/ivgn/product/10787018

AP1.2 1 100kp DNA Ladder, Invitrogen
`   http://products.invitrogen.com/ivgn/product/15628019

AP1.31   OneShot© Top10 chemically competent cells (Invitrogen C4040-10)
http://products.invitrogen.com/ivgn/product/C404010

AP1.4 XL10-Gold ultracompetent Cells (Stratagene C- 200314).
http://www.freewebs.com/labjuan2/XL10%20competent%20cells%20STRATAGENE.pdf

AP1.5 Miniprep (Qiagen Spin Miniprep kit)- Handbook
http://www.qiagen.com/literature/handbooks/literature.aspx?id=1000248

AP1.6 Maxiprep protocol see appendix Qiagen High speed Maxiprep kit
http://www.qiagen.com/products/plasmid/qiagenplasmidpurificationsystem/hispeedplasmidmidikit.aspx?rp=1000096&rpg=0

AP1.7 Gel purification, Qiagen Gel purification kit
http://www.qiagen.com/products/dnacleanup/gelpcrsicleanupsystems/qiaquickgelextra_ctionkit.aspx?rp=1000252&rpg=0

AP1.8 PCR Purification
http://www.qiagen.com/products/dnacleanup/gelpcrsicleanupsystems/qiaquickpcrpurificationkit.aspx?rp=1000254&rpg=0

AP1.9 SuperScript RT (Invitrogen)
http://www.invitrogen.com/site/us/en/home/Products-and-Services/Applications/Nucleic-Acid-Amplification-and-Expression-Profiling/RT-PCR/superscript-iii-first-strand-synthesis-system-for-rt-pcr.html

AP1.10 Phusion high fidelity PCR kit, Finnzymes F-553S/L
http://www.finnzymes.com/pcr/phusion_high_fidelity_pcr_kit.html

AP1.11 Mouse total RNA master Panel (Clontech 636644)
http://www.clontech.com/GB/Products/cDNA_Synthesis_and_Library_Construction/RNA/Total_RNA_Mouse/15_Tissues?sitex=10030:22372:US

AP1.12 Fantom CDNA clone
http://www.dnaform.jp/products/fantom/pd f/FANTOM-PX-PY-PZ.pdf

AP1.13 pcDNA3 with multiple cloning sites ,Invitrogen
http://products.invitrogen.com/ivgn/product/V79020

AP1.14 SAP, Alkaline Phosphatases , Roche
http://www.mundocaracol.com/laboratorio/Docs/protocols/SAP_Roche.pdf

AP1.15 pEGFP-N1
http://www.pkclab.org/PKC/vector/pEGFPN1.pdf

AP1.16 DreamTaq Green DNA polymerase kit, Fermentas
http://www.fermentas.de/product_info.php?info=p1600

CV - Jennifer König

Address:	65 Camden Road, Camden Town, London NW1 9EU
Phone:	07867933453
Email:	jennifer.koenig@gmx.at, j.koenig@wibr.ucl.co.uk
Date of birth:	07.07.1986
Nationality:	Austrian

RESEARCH EXPERIENCE

Nov 2010 – July 2011

Master Thesis, University College London

Department of Experimental Medicine, Molecular Nociception Group

Project title	Post- transcriptional regulation of SCN9A: an antisense transcript and RNA editing study
Description	The aim of this project is to ascertain whether the SCN9A mRNA undergoes RNA editing and hence alters the encoded protein sequence of Nav1.7
Techniques	Detection and amplification of SCN9 antisense mRNA
Supervisor	Prof.John N. Wood, PhD, FRS; James Cox. PhD;

July-August 2009

Internship, Centre of Brain Research

Department of Neuronal Cell Biology

Project title	Monitoring/ Detection of dendritically localized mRNA in hippocampal neurons
Description	The aim of the project was to investigate changes in P Body/RNP localisation and distribution due to chemical induced changes in neuronal activity. In addition to the localisation, the overall distribution of P- Bodies within a

neuron was detected. Therefore the RNP and P- body number within dendrites was determined as well as their spatial distribution.

Techniques By generating antisense probes complimentary to mRNAs (ARC, LimK) suspected to be crucial in dendritic development and P- Body marker. I performed several in situ hybridisations to compare RNA /P body distribution under various neuronal conditions (basal state, silenced and Glutamate) Real time imagining to determine mRNA / P body dynamics in hippocampal neurons.

Supervisor Prof Michael Kiebler, PhD; Georgia Vendra, PhD

April– May 2009

Internship, Center of Brain Research

Department of Neuroimmunology

Project title The role of CKLF1 in the EAE Mouse model of Multiple Sclerosis

Description Certain chemokine's preferentially enhance the migration of Th2 cells into the CNS.Chemokine like factor – 1 is a functional ligand of the CCR4 receptor and expressed on the surface of macrophages, dendritic cells and on the surface of Th2 cells. If Th2 cells are somehow recruited by chemokine like factor 1 they could function as potential key players in the shutdown of EAE by stimulating an immune protective pathway**.**

Techniques Purification and in vitro translation of CKLF1 which used to immunization of EAE mouse.

Supervisor Monika Bradl, PhD; Prof J. Lassmann, PhD

Nov – Jan 2009

Neuroscience Program - Lab Rotation training

Center of Brain Research, Medical University of Vienna

All Departments

Description Practical training to acquire commonly used techniques in Neuroscience

Techniques   Elisa, Fura Imaging**,** immunocytochemistry**,** in situ hybridisation

measurement of electrophysical properties of neurons, microscopy and

sample preparation Receptor binding studies, Mass- spectroscope,

SuperFusion

2005-2008

Lab Courses during the 1ˢᵗ Diploma – Vienna Biocenter

Lab courses

Molecular biology and Genetics I, IIA+ IIB, III, Cell biology

Biochemistry, Organic chemistry, Inorganic chemistry, Microbiology I, II

Techniques   Acquisition of basic knowledge and skills in molecular biology for example:

PCR, Western –, Northern blot, cloning, protein purification, DNA and RNA extraction,

Bradford, Mass-spectrometry

CAREER AIM

Since my undergrad I've been really passionate about Neuroscience and Genetics, in

particular RNA Biology. Recently I came to realise that I would love to further knowledge in

Bioinformatics and DNA sequencing.

EDUCATION

Master Thesis	**University College London**	2010-2011
	Molecular Nociception Group	
Masters	**University of Vienna**	2008-2010
	Lectures and lab courses in Molecular Neuroscience	
	Specialization: Neuroscience, Cell biology and	
	Molecular medicine	
	Université Aix- Marseille III	2009-2010

European exchange student. Following a course in cognitive and integrative Neuroscience

Undergrad	**University of Vienna**	2005-2008

1st Diploma in Molecular biology

Key aspect: Cell biology, Molecular biology, Neuroscience, ChemistryBiology, Grade: B;

High school	**Bundesoberstufenrealgymnasium (BORG**)	2001-2005

Grieskrichen, OÖ

A- Level with honour

INTERESTS

- Languages: fluent in German and English , French good but not fluent
- Travelling and Anthropology
- Art expositions
- Reading
- Salsa

WORK EXPERIENCE

Spring 2008   Sale advisor at H&M